PERGAMON

Archives of Oral Biology 43 (1998) 969–977

ARCHIVES OF ORAL BIOLOGY

Histogenesis of the chequered pattern of ivory of the African elephant (*Loxodonta Africana*)

E.J. Raubenheimer[a,*], M.C. Bosman[b], R. Vorster[a], C.E. Noffke[a]

[a]*Department of Oral Pathology, Faculty of Dentistry, Medical University of Southern Africa, P.O. MEDUNSA, 0204, Republic of South Africa*

[b]*Department of Anatomy, Medical University of Southern Africa, P.O. MEDUNSA, 0204, Republic of South Africa*

Accepted 16 June 1998

Abstract

This study aimed to propose a hypothesis on the events which lead to the development of the characteristic chequered pattern of elephant ivory. Twenty fragments of ivory and six elephant tusks were obtained through the National Parks Board of South Africa. Polished surfaces were prepared in sagittal and longitudinal planes and the characteristics of the distinctive chequered pattern described. Light- and electron-microscopical techniques and image analyses were employed to determine the morphological basis of the pattern and to describe the spatial distribution, density and morphology of the dentinal tubules. These investigations showed that the distinctive pattern was the result of the sinusoidal, centripetal course followed by dentinal tubules. The apical, slanted part of the sinusoidal curve is the result of the centripetally moving odontoblast, which, during formation of ivory, progresses towards the centre of the tusk on a decreasing circumference. It is suggested that this leads to cell crowding, increased pressure between odontoblasts and subsequent apical movement of their cell bodies, cell degeneration and fusion. Odontoblastic degeneration and fusion probably relieve the pressure between the crowded odontoblasts by reducing their numbers and the remaining odontoblasts now orientate their centripetal course towards the tip of the tusk, thereby forming the anterior-directed part of the sinusoidal path of the tubule. As odontoblasts progress centripetally the diameter of the pulpal cavity decreases further and the processes of apical movement, fusion and degeneration of odontoblasts are repeated. This occurs until the pulpal cavity is obliterated.

Keywords: Elephant ivory; Dentinal tubules; Dentine; Odontoblastic movement

1. Introduction

Elephants are characterized by a highly pneumatic skull with a premaxilla that descends vertically, bearing the roots of the paired tusks, which represent enormously enlarged maxillary incisors. The growth of the tusk is continuous throughout life and its size at any age is dependent on the sex of the animal, the rate of attrition and breakage of the tooth, as well as genetic and environmental factors (Hall-Martin, 1982). The record length of a single tusk is 3.51 m and record weight 117 kg. The bulk of the tusk consists of ivory (or dentine), ensheathed by a layer of cementum (Sikes, 1971).

The unique chequered pattern of polished ivory, which has not been described in great detail in the literature (Sognnaes, 1960; Miles and Boyde, 1961; Sikes, 1971; Raubenheimer et al., 1990), has made it a sought-after product in the manufacturing of jewellery and other works of art. Our purpose now was to pro-

* Corresponding author. Department of Oral Pathology, Medical University of Southern Africa, Box D24, P.O. MEDUNSA, 0204. Fax: (012) 521 4838; Email: ejraub@mcd4330.medunsa.ac.za.

0003-9969/98/$ - see front matter
PII: S0003-9969(98)00077-6

pose a hypothesis on the histogenesis of the unique chequered pattern of elephant ivory.

2. Materials and methods

Twenty fragments of ivory and five tusks of African elephant (*Loxodonta Africana*) and a developing tusk of a 22-month fetus were obtained through the National Parks Board of South Africa. The ivory was harvested from animals that had died as a result of natural causes or as part of the population-control programme of the National Parks Board. The fetal tissue was obtained within 20 min of death. The biopsies were taken with a sharp scalpel from the peripulpal ivory of the proximal part of the tusk, cut in thin slices and then fixed in 10% phosphate-buffered formalin at 21°C.

The five tusks, with masses between 0.7 and 9.3 kg, were sectioned and polished in sagittal and coronal planes. The morphological characteristics of the chequered pattern were described on polished surfaces prepared in both planes. Irregularities affecting the pattern were noted.

Ground sections were prepared parallel and perpendicular to the long axis of 12 different fragments of ivory by cutting 300-μm thick slices of ivory from the respective planes with a rotating diamond saw. The thick slices were fixed to glass slides with methylmethacrylate cement and ground to a thickness of approx. 40 μm on a rotating disc utilizing different grades of diamond pastes. The ground sections were covered with glass cover-slips after debridement with a weak acid solution (0.1 M HCl) and a soft brush, and examined by transmission light microscopy under standard illumination.

Standardized techniques for the preparation of scanning electron micrographs of hard tissues were employed to visualize the morphology and distribution of dentinal tubules of six different tusks when viewed from the pulpal surface of the ivory. The presence of light or dark bands was noted during the preparation of an additional 10 sections at different levels perpendicular to the long axis of the tubules. The levels were selected so that five sections passed through light bands and five through dark bands. All surfaces were cleaned before scanning with a 0.1 M HCl solution and a soft brush, and flushed with deionized water to

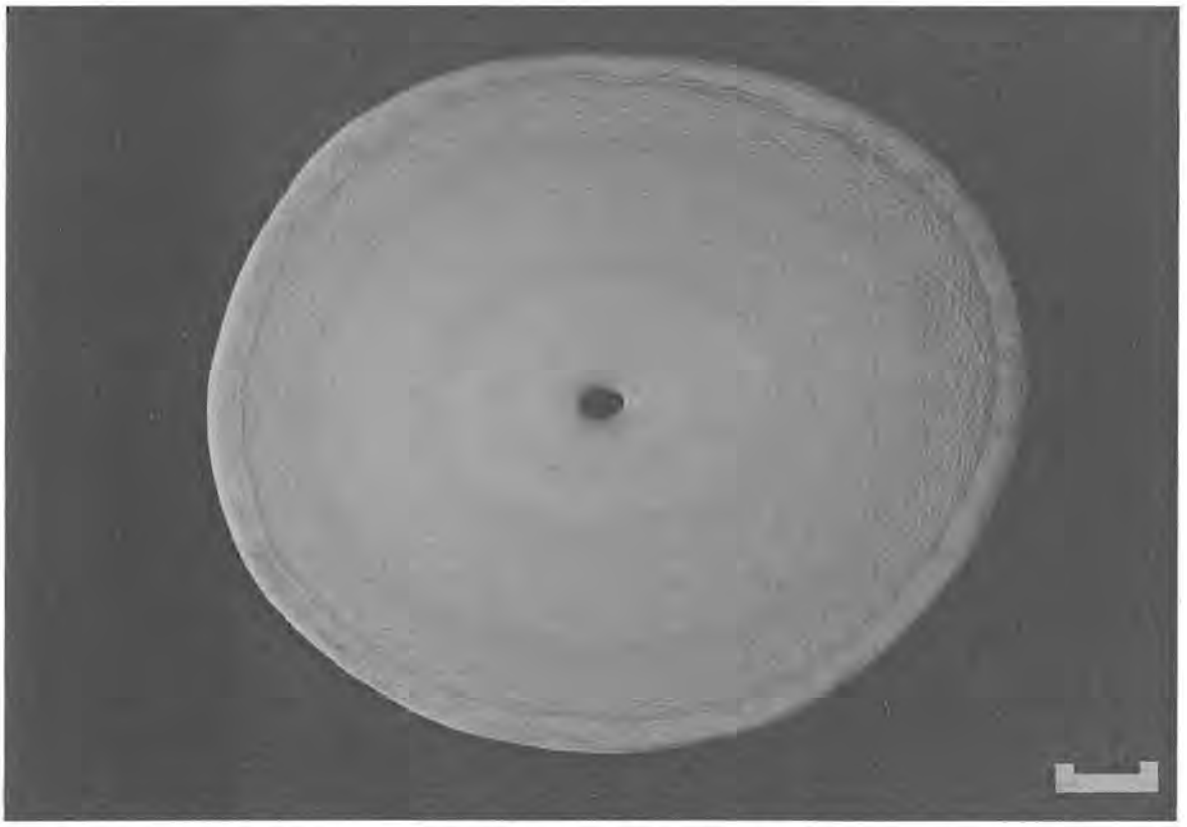

Fig. 1. Cross-section through the solid part of a tusk. Note the undulating course the cementum–ivory junction follows and the geometric chequered pattern (bar = 4 cm).

remove debris. The distance between tubules was expressed as the smallest linear measurement between two adjacent tubules and the tubule density as the number of tubules per mm^2. At least 10^3 tubules were counted for each measurement. An image analyser was used (Flexible Image Processing System, CSIR, Pretoria) and findings were subjected to the Student's *t*-test for unequal variances.

3. Results

The entire outer surfaces of the tusks were covered by a layer of cellular cementum. Ivory was exposed on the working surfaces of erupted tusks through cemental abrasion. The cementum–ivory junction was visible as a dark, concentric ring demarcating the peripheral border of the ivory. In cross-sections through the tusk, the cementum–ivory junction followed an undulating circular course, forming irregular excrescences alternating with shallow convexities or concavities (Fig. 1). The excrescences were more pronounced in tusks with smaller diameters. Occasional invaginations of cementum, which were 2–3 mm deep, were present in the outer layer of the ivory. The external contour of the cementum followed the morphology of the cementum–ivory junction, resulting in longitudinal and parallel ridges and troughs had been visible upon external examination of the tusks. These ridges and troughs had been abraded away on the anterior and more exposed surface of the tusk. The pulpal surface of the ivory was smooth and the pulpal cavity conical in shape, with the tip of the tusk composed of solid ivory and the apical foramen wide open (Fig. 2).

The unique chequered pattern was evident on polished surfaces of cross-sections through the tusk (Fig. 1). The pattern consisted of two systems of alternating light and dark lines which started adjacent to the cementum. One system swept clockwise and the other anticlockwise towards the centre of the tusk, intersecting at regular intervals. The chequered pattern corresponded to parallel alternating light and dark lines evident on polished surfaces prepared in the sagittal plane (Fig. 3). The cementum–ivory junction was straight when viewed in this plane. Planes of fracture through ivory tended to follow the contours of the dark bands.

The outermost layer of ivory (mantle ivory) was between 40 and 80 μm thick and consisted of irregularly spaced dentinal tubules which were slanted api-

Fig. 2. Tusk of an elephant bull (top) and cow (bottom). Note the parallel ridges and troughs on the posterior surface of the bull's tusk (arrows). The broken line in the lower tusk represents the wall of the conical pulpal cavity (bar = 10 cm).

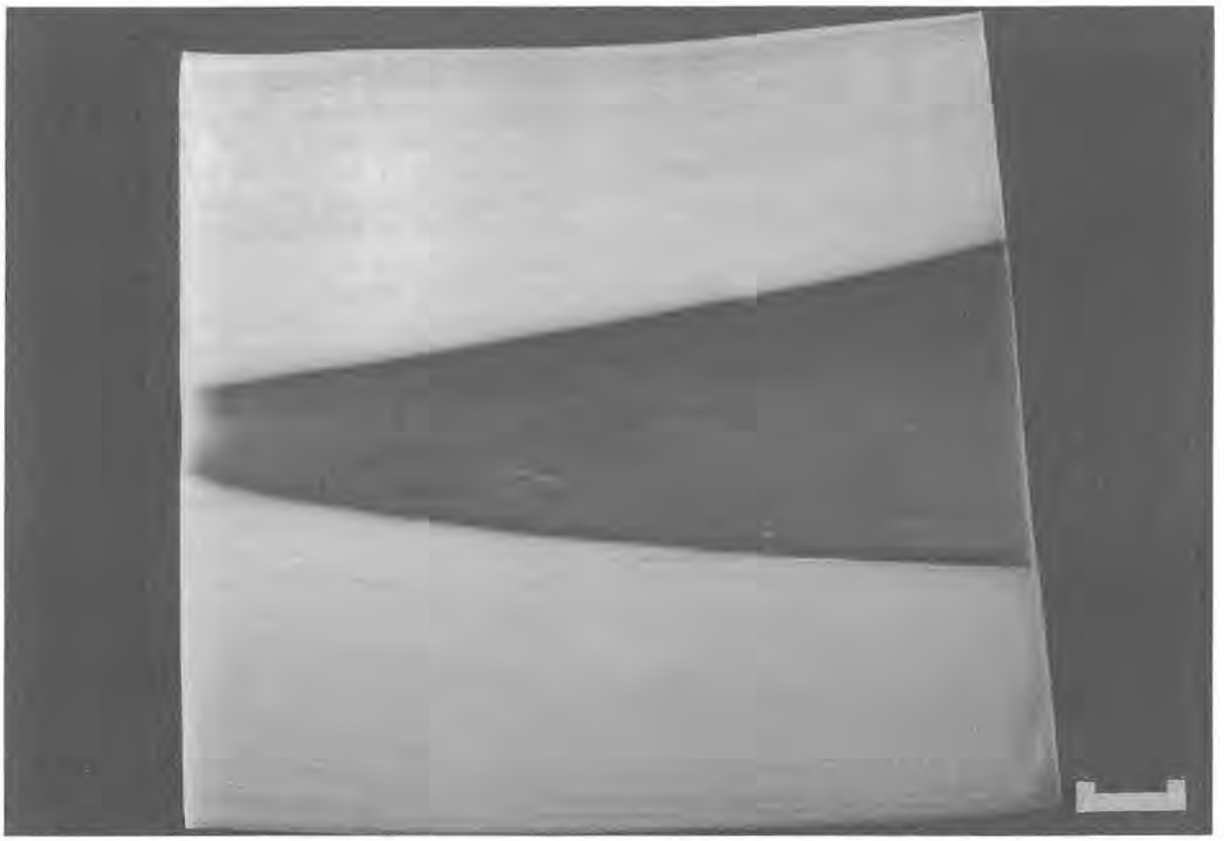

Fig. 3. Sagittal section through a tusk. Note the conical pulpal cavity and parallel light and dark bands in the ivory, the latter of which are evident in the outer third (bar = 4 cm).

cally at a sharp angle to the cementum–ivory junction (Fig. 4). These tubules appeared to branch extensively, a feature which was best observed when focusing at different planes in the section. Morphologically, the mantle ivory resembled the granular layer of human radicular dentine. After passing through the mantle ivory, the tubules became more regularly spaced and gradually changed their course by curving towards the tip of the tusk. This curvature was the beginning of the regular, sinusoidal course followed by the dentinal tubules in a pulpal direction and was evident only in sections prepared in the sagittal plane. The convexities and concavities of this sinusoidal pattern corresponded to the alternating light and dark bands seen macroscopically on surfaces prepared in the sagittal plane (Fig. 5). The dark bands correlated with that part of the dentinal tubules that curved apically. On high-power magnification, many dentinal tubules appeared to end blind and scattered tubules appeared to fuse forming one tubule (Fig. 6). The blind-ending tubules were more frequent in the dark bands in ivory (16 blind-ending tubules per 100 tubules, SD 7 tubules) than in the light bands (6 blind-ending tubules, SD 3 tubules) as measured over 2500 tubules in each of the dark and light bands, respectively ($p < 0.001$). The process of apparent fusion involved the main dentinal tubule and was distinct from the fine lateral branches that seemed to anastomose with those of adjacent tubules. Demineralized sections of newly formed ivory in the fetal tissue showed crowding of distally slanted odontoblasts and scattered pyknotic cells, highly suggestive of individual cell death (Fig. 7).

Scanning electron microscopy showed that the pulpal openings of the dentinal tubules were oval with the greatest dimension parallel to the long axis of the tusk. The indentations of scattered cell bodies, which appeared larger than those of adjacent cells and in which two distinct tubules terminated, were focally evident (Fig. 8). Dentinal tubules were closer packed in areas where they curve apically (i.e., the dark bands) (mean distance $4.6 \pm 1.7\ \mu m$ SD) than in the part of the tubule that curves towards the tip of the tusk (i.e., the light bands) (mean distance $7.2 \pm 2.8\ \mu m$ SD). This difference was significant ($p < 0.001$).

Fig. 4. Microscopic appearance of mantle ivory. Note the sharp, apical-directed slant of the first part of the dentinal tubules (arrows) (bar = 50 μm; magnification ×200).

4. Discussion

The cell responsible for the formation of ivory (or dentine) is the odontoblast. Odontoblasts are derived from the mesenchyme of the adjacent dental papilla, and, after differentiation and cytoplasmic maturation, they move in a centripetal direction and deposit ivory along their pathway. The tip of the conical pulp soon becomes solid and lengthening of the apical edge coincides with forward displacement of the tusk.

The morphological characteristics of ivory can be explained by events which result from the differentiation and centripetal movement of the odontoblast. When the first ivory is formed, cuboidal odontoblasts lie tightly packed around the periphery of the pulp. The circumference of the circular plane along which they lie is $2 \times \pi \times R$. As the odontoblast moves centripetally, a reduction in the radius (or R) by one unit would result in a decrease of the circumference by 6.28 units. Because of this significant reduction in the circumference during centripetal movement of odontoblasts, they probably soon become more tightly packed along their course and the lateral pressure between them increases. Differentiation of odontoblasts, which is characterized by an increase in the volume of cytoplasmic organelles (Sasaki and Garant, 1996) and resultant cell enlargement, may also contribute to odontoblastic crowding during the early stages of dentinogenesis. During the first phase of formation of the early (most peripheral) ivory and before mineralization takes place, the pressure caused by cell crowding and cytoplasmic enlargement probably results in the undulating course followed by the ivory–cementum junction. That course accommodates more odontoblasts per unit length than would a regular curve, thereby relieving this pressure. The reduction of the circumference per unit movement of the odontoblast on the radial axis is greater in tusks with a smaller diameter and the undulating course of the ivory–cementum junction is therefore more pronounced in smaller tusks. After mineralization of the first ivory has taken place, further folding of the ivory–cementum junction fails to occur, owing to the rigidity which the deposition of mineral salts introduces to the newly formed ivory. This initiates a new set of events which accommodates odontoblastic crowding during their centripetal movement. These events result in the sinusoidal pathway followed by the odontoblasts when viewed in a sagittal plane along their course toward the centre of the tusk.

The pulpal cavity of the tusk is conical when viewed in a sagittal plane and confined on all aspects by mineralized ivory except for the large apical opening through which the vascular and nerve supplies pass. The only means by which the growing pressure between centripetally moving odontoblasts on an ever-decreasing pulpal perimeter can be accommodated is through apical movement of the odontoblastic cell mass or a reduction in the number of odontoblasts. A reduction in the number of odontoblasts could be achieved through odontoblastic cell death or fusion. There is morphological evidence that all these processes occur during the formation of elephant ivory. The following features favour this hypothesis:

1. Acute slanting of the first part of the odontoblastic processes towards the apical aspect of the tusk is indicative of a force which displaces the odontoblasts bodily and in an apical direction during early centripetal movement from the ivory–cementum junction.

Fig. 5. Microscopic appearance of the regular sinusoidal course followed by the odontoblastic tubules when viewed in the sagittal plane. Note the alternating dark and light bands, the former corresponding with the apically orientated slant of the tubules (bar = 120 μm; magnification ×80).

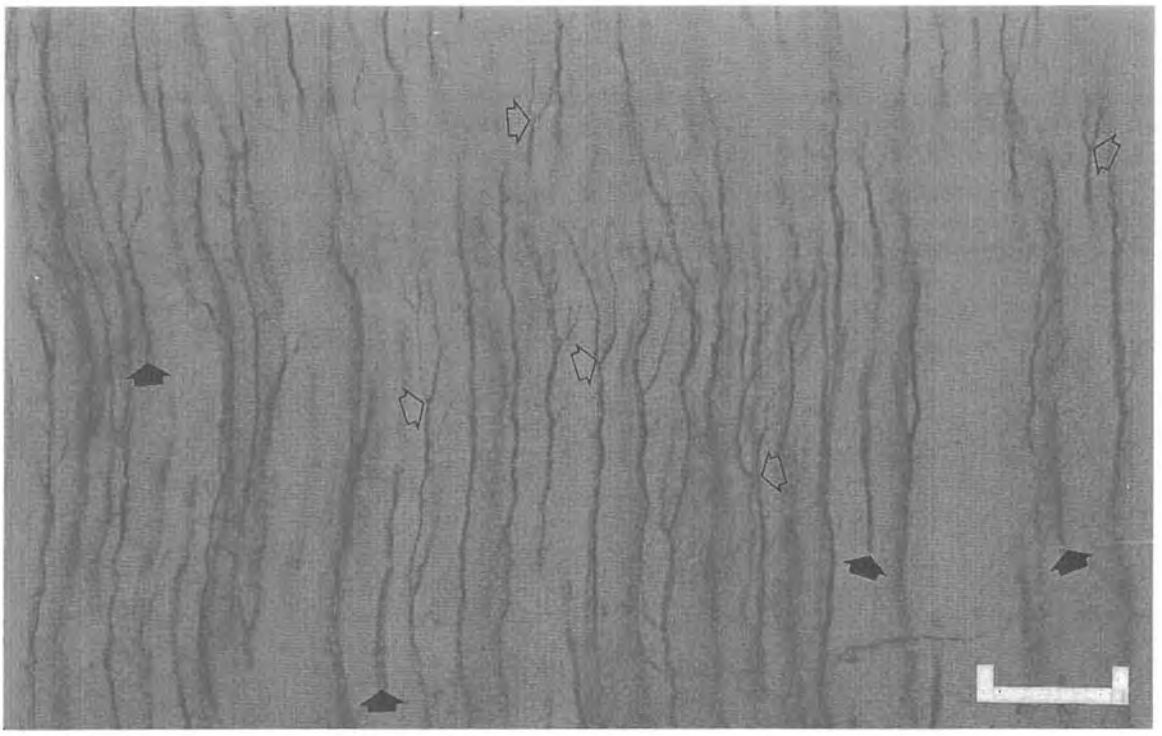

Fig. 6. Blind-ending tubules (dark arrows) and fusing tubules (open arrows) in the dark bands of ivory (bar = 20 μm; magnification ×600). The pulpal cavity is orientated towards the lower margin of the figure.

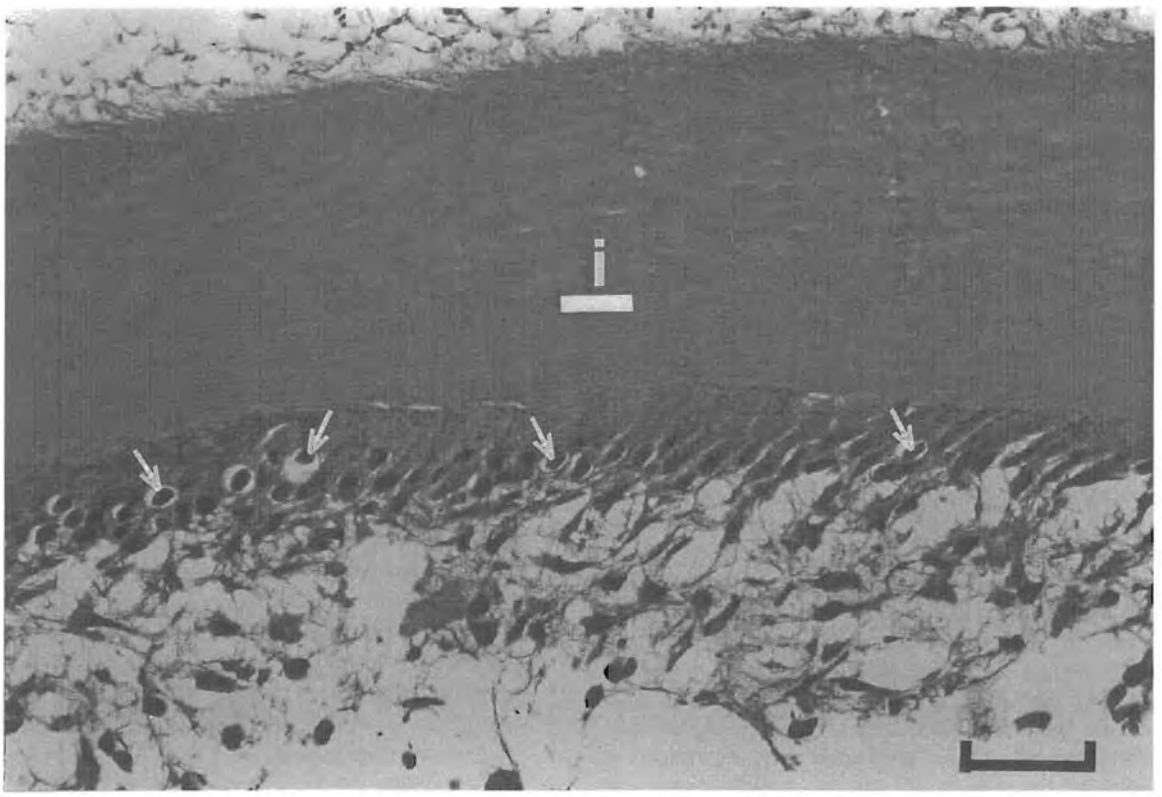

Fig. 7. Apically slanted odontoblasts lining the pulpal surface of newly formed ivory (i). Note scattered pyknotic odontoblasts (arrows) (H&E stain; bar = 40 μm; magnification ×300).

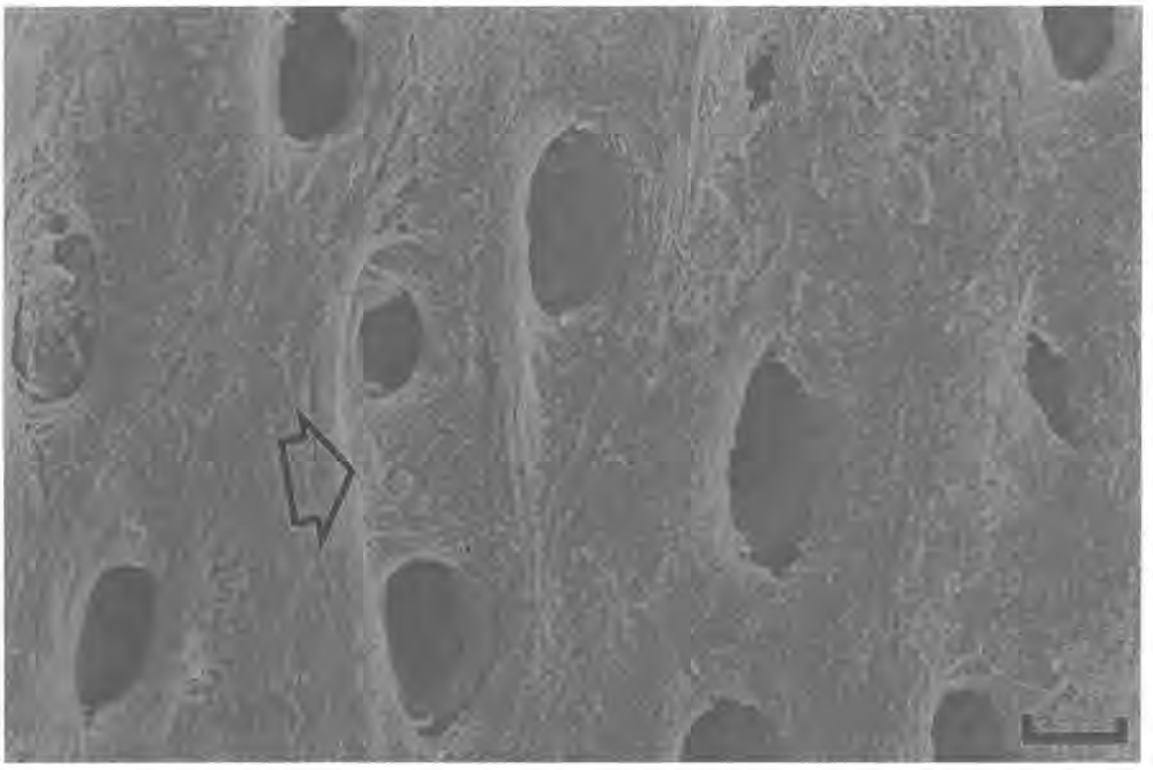

Fig. 8. Scanning electron micrograph of the pulpal surface of ivory. Dentinal tubules are oval with their long axis parallel to the axis of the tusk. Note the large, unilocular indentation (arrow) into which two tubules open (bar = 3 μm).

This displacement is probably due to cell crowding, which is likely to be the result of enlargement of differentiating cells as well as a progressive reduction of the pulpal circumference.

In human dentine major, fine and microbranches have been described along the course of dentinal tubules. The major branches are characteristically Y-shaped, dichotomous or trichotomous, with their general direction being generally parallel, whereas the other forms of branching extend from the main tubules at about 45° (Mjör and Nordahl, 1996).

2. The morphological phenomenon of fusion of dentinal tubules probably represents fusion of odontoblastic cell bodies. Fusing tubules feature in regions represented macroscopically by dark bands and coincide with the point at which the sinusoidal curve begins to turn towards the tip of the tusk. In the subsequent portion of the centripetal course of the odontoblasts (i.e., the light bands), fusion has been shown to be less extensive. This indicates that distinct phases of odontoblastic fusion are triggered through pressure which builds up between the cells during their centripetal course. It is proposed that odontoblastic fusion alleviates cell crowding by reducing the number of cells on a rapidly decreasing pulpal circumference.
3. Microscopic examination of thin sections through ivory indicates that more tubules appear to end blindly when entering the posteriorly slanted portion of their centripetal course. This, together with the scattered pyknotic odontoblasts seen in sections of rapidly fixed fresh specimens of developing tusks, indicates that crowding with resulting intercellular pressure may in fact induce degeneration of individual odontoblasts. The effect of this would be to reduce the number of odontoblastic cell bodies on a progressively decreasing pulpal circumference, thereby making more space available for the remaining odontoblasts.
4. In planes where the odontoblast cell bodies slant posteriorly, and where crowding of cells with fusion and cell death take place, the dentinal tubules are more closely packed. This is supported by the histomorphometric findings, which clearly indicate that dentinal tubules are closer packed in zones where they curve towards the tip of the tusk (i.e., the darks bands) than in those areas where the tubules curve anteriorly (i.e., the light bands). The reduced volume of mineralized ivory and increased density of tubules in the dark bands probably result in inherent planes of weakness. This could be one of the

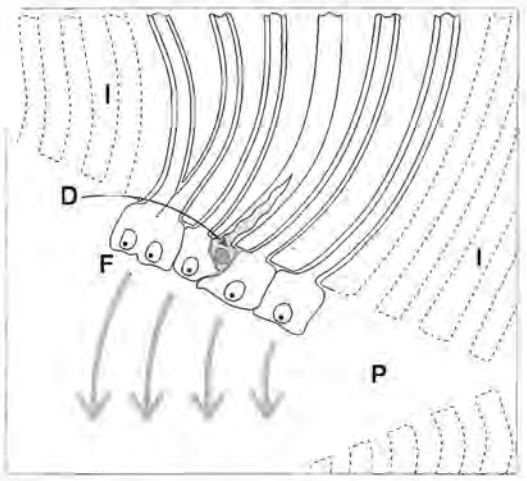

Fig. 9. Schematic representation of part of the sinusoidal pathway followed by the dentinal tubule in its centripetal course. Note the crowding of odontoblasts, odontoblastic fusion (F) and degeneration (D) (I, ivory; P, pulpal cavity).

reasons why planes of cleavage in fractured ivory tend to follow the contours of the dark bands.

A scanning electron-microscopic investigation of human dentinal tubules (Garberoglio and Brännström, 1976) showed that tubule density increases towards the pulp. Their counts ranged from a mean of 19,000 tubules per mm^2 3.1–3.5 mm from the pulp to 45,000 tubules per mm^2 in dentine 0.1–0.5 mm from the pulp. This increase in tubule density as the odontoblast progresses towards the human dental pulp is indicative that the human odontoblasts are subjected to the same forces as proposed in the elephant.

5. Scanning electron microscopy of the pulpal surface of ivory shows large, unilocular indentations (possibly representing one large, fused cell body) with two distinctly separate tubules (perhaps representing the cytoplasmic processes of two separate cells) permeating the ivory. These features support our hypothesis that odontoblastic fusion occurs during their centripetal movement.
6. The oval shape of the dentinal tubule when viewed perpendicular to its course, is morphological evidence of circumferential pressure which builds up between centripetally moving odontoblasts.

The processes of odontoblastic crowding, followed by a bodily apical movement of odontoblasts and a relief of the intercellular pressure through cell fusion and death, with a subsequent change in the direction of movement of the cell body of the remaining odontoblasts, are probably responsible for the regular sinusoidal course followed by the odontoblast in its centripetal course during the formation of ivory (Fig. 9). The sinusoidal course of the dentinal tubule is reflected as parallel and alternating light and dark bands which are seen on polished surfaces prepared along the long axis of the tusk. The light and dark bands were found to be the result of the varying compactness of dentinal tubules between the sectors of the sinusoidal curve of the tubules that slant towards the tip of the tusk or its apex, respectively. The scattering of light, which was proposed by Miles and Boyde (1961) as an explanation for the bands, probably has less of a role in the morphogenesis of the pattern. On cross-sections, the chequered pattern is a reflection of the alternating light and dark bands seen on surfaces prepared in length. This implies that when the layer of odontoblasts is viewed from a radial perspective, apical movement of the odontoblasts with curving of the dentinal tubules does not occur at the same time but rather as a wave that spreads circumferentially along the layer of odontoblasts.

Acknowledgements

Appreciation is expressed to Mrs C. Begemann for editing the manuscript.

References

Garberoglio, R., Brännström, M., 1976. Scanning electron microscopic investigation of human dentinal tubules. Arch Oral Biol 21, 355–362.

Hall-Martin, A., 1982. Kruger's tuskers. Afr Wildl. 35 (1), 65–88.

Miles, A.E.W., Boyde, A., 1961. Observations on the structure of elephant ivory. J Anat (Lond) 95, 450 (Abstract).

Mjör, I.A., Nordahl, I., 1996. The density and branching of dentinal tubules in human teeth. Arch Oral Biol 41, 401–412.

Raubenheimer, E.J., Dauth, J., Dreyer, M.J., Smith, P.D., Turner, M.L., 1990. Structure and composition of ivory of the African elephant (*Loxodonta africana*). S A J Science 86, 192–193.

Sasaki, T., Garant, P.R., 1996. Structure and organisation of odontoblasts. Anat Rec 245, 235–249.

Sikes, S.K., 1971. The natural history of the African elephant. Part I. Weidenfeld and Nicholson, London, pp. 1–184.

Sognnaes, R.F., 1960. The ivory core of tusks and teeth. J Clin Orthopaedics 17, 43–61.

PERGAMON

Archives of Oral Biology 45 (2000) 983–986

Archives of Oral Biology

www.elsevier.com/locate/archoralbio

Early development of the tush and the tusk of the African elephant (*Loxodonta africana*)

E.J. Raubenheimer *

Medical University of Southern Africa, Department of Oral Pathology, P.O. Box D24, Medunsa 0204, South Africa

Accepted 16 May 2000

Abstract

This early development was studied from a serial histological sections of eight elephant embryos with masses varying between 1 and 240 g. The tush and the tusk develop from one tooth germ in a deciduous to permanent tooth relation. In order to study the mineralization of the dental organ of the tush and cap and bell stage of the tusk, embryos older than 3-months' gestation (weighing more than 250 g) would be required. © 2000 Elsevier Science Ltd. All rights reserved.

Keywords: Tusk; Tush; Elephant; Embryology

1. Introduction

The tusk of the African elephant, *Loxodonta africana*, is a maxillary incisor tooth, which grows continuously throughout life. In contrast to the Asian elephant, *Elephas maximus*, tusks of the African elephant are well developed in both the sexes, with those of males being longer, more conical and thicker for their length than those of females (Pilgram and Western, 1986). Elephant calves exhibit a tooth adjacent to the tusk, which is commonly referred to as the 'tush' (Sikes, 1971). The tush does not erupt, but is pushed aside by the growing tusk and is eventually resorbed in the surrounding tissue (Raubenheimer et al., 1994). Gestation lasts an average of 22 months and the tusk erupts approximately 1 year after birth (Sikes, 1971; Ricuitti, 1980). Although it has been accepted by most that the tusk is the permanent successor to the 'deciduous' tush (Sikes, 1971; Raubenheimer et al., 1994), Anthony, 1933 regarded the tush as a rudimentary incisor belonging to a neighbouring position to the tusk. Furthermore, palaeontological data indicate that these two teeth are not homologous and both pairs of incisors of Proboscideans are teeth of the primary (or deciduous) dentition with no dental replacement by a permanent tooth (Tassy, 1987). No study has been executed on the early embryological development of the tush and tusk of the elephant.

The purpose of this study was to establish whether the tush and the tusk of the African elephant represent separate teeth or develop from one tooth germ in a deciduous to permanent tooth relation.

2. Materials and methods

Eight elephant embryos were harvested during the population control programme of the Kruger National Park (de Vos, 1983). All embryos were obtained from cows with tusks, except for the 48.4-g embryo, which had a tuskless mother. The masses (sex and gestational age; Sikes, 1971) of the embryos were 1 g (unknown, less than 1 month), 6.5 g (unknown, 1 month), 48.4 g

* Corresponding author. Tel.: +27-12-5214838; fax: +27-12-5214838.

E-mail address: ejraub@medunsa.ac.za (E.J. Raubenheimer).

PII: S0003-9969(00)00068-6

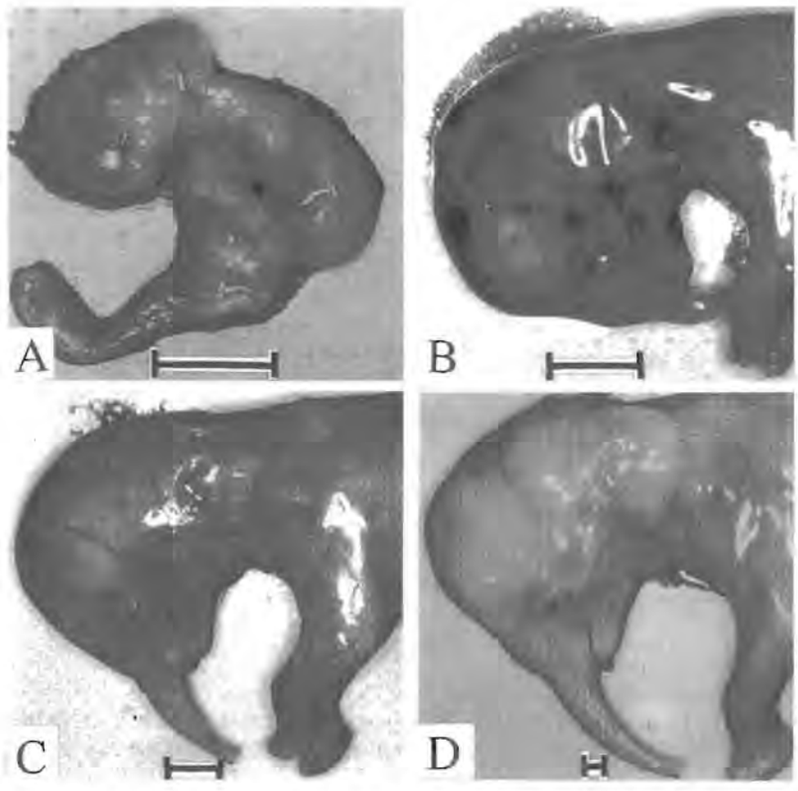

Fig. 1. External features of four of the elephant embryos, (a) 1 g; (b) 6.5 g; (c) 48.4 g and (d) 94.4 g. Bar = 1 cm.

(unknown, 2 months), 93 g (male, 2–3 months), 94.4 g (male, 2–3 months), 107 g (female, 2–3 months), 136 g (male, 2–3 months) and 240 g (male, 3 months). The heads of all but the smallest were hemisected, radiographed, fixed in buffered formalin and processed for routine light microscopy. The head of the 1-g embryo was not hemisected. Serial sections were cut of each in the sagittal plane and stained with haematoxylin and eosin. The developmental chronologies of the lamina dentalis and the primordia of the tush and tusk were recorded through microscopic examination.

3. Results

On external examination, the eye placodes and stomodeal openings were macroscopically evident in all embryos and only the 1-g specimen did not show evidence of a developing trunk (Fig. 1). Radiological examination failed to identify mineralized tissues in the nasomaxillary complexes of the 1 and 6.5-g embryos. The earliest stage at which it was possible to identify the os incisivum (the part of the nasomaxillary complex in which the tush and tusk develop) radiologically was in the 48.4-g embryo. The os incisivum in the 136-g embryo showed a central radiolucent area where early development of the tush was taking place.

Microscopic examination of the 1-g embryo showed the stomodeum lined by primitive epithelium. No dental lamina could be identified by serial sectioning. The early development of the dental lamina of the tush was present in the 6.5-g (1 month) embryo. Ectomesenchyme aggregated densely around the tip of the dental lamina at this stage (Fig. 2). Formation of the cap stage of the dental organ of the tush was evident in

Fig. 2. Low-power microscopic view of the stomodeum of the 6.5-g embryo; note the dental lamina (arrow) growing towards the os incisivum (*). Haematoxylin and eosin, 80 × .

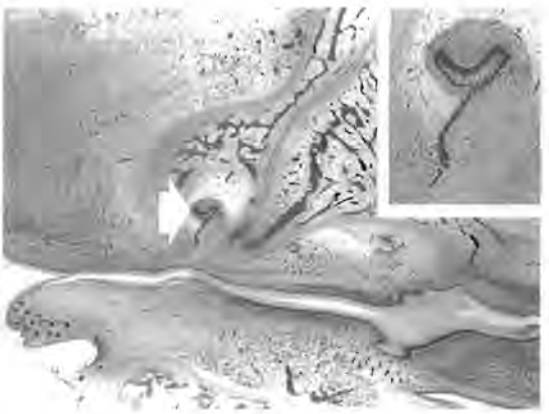

Fig. 3. Cap stage of the tush of the 48.4-g embryo (arrow); note the formation of bone around the dental organ. Haematoxylin and eosin, 30 ×. Inset: Higher magnification of the dental organ 80 ×.

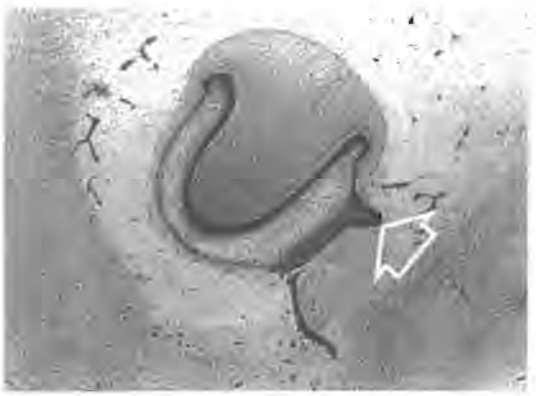

Fig. 4. Bell stage of the dental organ of the tush of the 136-g embryo; note the formation of the bud for the development of the of the tusk which originates from the external epithelial layer of the dental organ of the tush (arrow) 200 ×.

sections of the 48.4-g embryo. The dental lamina of the tush was partially intact and ectomesenchymal aggregates formed the dental follicle and dental papilla. Formation of the bone of the os incisivum was present around the dental organ (Fig. 3). The 94.4-g embryo showed loss of continuity of the dental lamina; development of the bell stage of the dental organ of the tush was evident in sections of the 136-g embryo. At this stage, further epithelial proliferation of the external enamel epithelium of the bell stage of the tush formed the bud stage of the successional tooth germ, the tusk (Fig. 4). Ameloblastic and odontoblastic differentiation with early depositioning of enamel and dentine in the dental organ of the tush were evident in the 240-g specimen.

4. Discussion

The bud stage of the tusk of the African elephant has its origin from the cap stage of the developing tush. The tush and the tusk of the African elephant develop in succession and have a deciduous to permanent tooth relation. These findings are contrary to those of Anthony (1933) and Tassy (1987), who proposed the tush and tusk to represent separate teeth of the same series of incisors. My observation is supported by a previous publication (Raubenheimer et al., 1994) on the later embryologic development of the tush, which, in a dissected specimen, had shown the fully developed tush to be located anterior to the follicle of the developing tusk. After completion of development, the tush frequently fails to erupt, is pushed aside by the growing tusk and is eventually resorbed. The displacement of the tush by the enlarging tusk, which is clearly evident in dissected specimens of newly born elephant calves, may have prompted Anthony (1933)in his observation that the tush develops adjacent to and separately from the tusk.

Although the tush could be viewed as a non-functional vestigial dental remnant, it plays an important part in the development of the tusk. The primordium of the tush not only provides the anlage for the development of the tusk, but also orientates the dental organ of the tusk in the os incisivum and creates a pathway for the eruption thereof. It furthermore delays the onset of development of the tusk by several months during the first trimester of pregnancy. This delay may be important in retarding the eruption of the tusk until well after birth, thereby facilitating breast feeding during the first year of life.

Acknowledgements

The author wishes to acknowledge C.S. Begemann for secretarial assistance and the National Research Foundation for financial support.

References

Anthony, R., 1933. Recherche sur les incisives superieures des elephantidea actueles et fossils. Arch. Mus. Natn. Hist. Nat. Paris 10, 61–124.

de Vos, V., 1983. Management of large animals in African conservation areas. In: Owen-Smith, M.A. (Ed.), Proceedings of a Symposium held in Pretoria, 29–30 April 1982. Haum, Pretoria, pp. 213–232.

Pilgram, T., Western, D., 1986. Inferring the sex and age of African elephants from tusk measurements. Biol. Conserv. 36, 39–52.

Raubenheimer, E.J., Van Heerden, W.F.P., Van Niekerk, P.J., de Vos, V., Turner, M.J., 1994. Morphology of the deciduous tusk (tush) of the African elephant (*Loxodonta africana*). Arch. Oral Biol. 40 (6), 571–576.

Ricuitti, E.R., 1980. The ivory wars. Anim. Kingd. 83 (1), 6–58.

Sikes, S.K., 1971. The Natural History of the African Elephant. Weidenfeld and Nicholson, London, pp. 8–111.

Tassy, P., 1987. A hypothesis on the homology of proboscidean tusks based on paleontological data. Am. Mus. Novit. 2895, 1–18.

Development of the tush and tusk and tusklessness in African elephant (*Loxodonta africana*)

E. J. RAUBENHEIMER

Raubenheimer, E.J. 2000. Development of the tush and tusk and tusklessness in the African elephant (*Loxodonta africana*). *Koedoe* 43(2): 57–64. Pretoria. ISSN 0075–6458.

The embryologic development of the tush and tusk of the African elephant was studied by means of serial histologic sections prepared from elephant embryos with masses varying between 1g and 240 g. Statistics on tusklessness obtained during a four year population control programme in the Kruger National Park were analysed and compared with those reported in other elephant reserves in Southern Africa. Maxillae of eight elephant embryos, the maternal histories of which were available in six cases, were radiographed, dissected and examined microscopically. This study has shown that the tush and tusk develop from one tooth germ in a deciduous to permanent tooth relationship. Tusklessness was found to be unilateral or bilateral and associated with either the absence or presence of a tush. The possible causes of the differences in the frequency of bilateral tusklessness in different elephant populations are discussed.

Key words: African elephant, embryology of tusk and tush, tusklessness.

E. J. Raubenheimer, Department of Oral Pathology, Medical University of Southern Africa, P.O. Medunsa, 0204, South Africa. (ejraub@medunsa.ac.za)

Introduction

The tusk of the African elephant (*Loxodonta africana*) is a pre-maxillary lateral incisor tooth which erupts at an age of approximately one year (Grzimek 1972). It is preceded by a deciduous incisor which is commonly referred to as the 'tush' (Sikes 1971). Although it has been accepted by most that the tusk is a permanent successor to the "deciduous" tush (Sikes 1971; Raubenheimer *et al.* 1995), Anthony (1933) regarded the tush as a rudimentary incisor belonging to a neighbouring position to the tusk. Paleontological data indicate that these two teeth are not homologous and incisors of Proboscideans are teeth of the primary (or deciduous) dentition with no dental replacement by a permanent tooth (Tassy 1987). The tush does not appear to erupt frequently and is pushed aside by growing tusk where it is resorbed in the adjacent tissue (Raubenheimer *et al.* 1995).

The tusk grows continuously throughout life, the size of which is important in determining the hierarchical position of a particular elephant in a herd. The most powerful cow, usually the largest tusker fulfils the role of the matriarch and determines the breeding pattern within her herd (Sikes 1971). Although large tusk-bearing elephant receive considerable attention in the literature (Hall-Martin 1981; Pilgram & Western 1986), little is known of those failing to develop tusks other than their low hierarchal status within the herd. In a study performed on foot in the Mana Pools Game Reserve in the Zambezi valley, 10 percent of 150 adult elephant were found to be tuskless. The tuskless elephant were divided in eight different groups, with one herd consisting of six tuskless elephant and only two with tusks. Amongst immature animals, 23 percent were found to be tuskless. This may indicate an increase in tusklessness in immature elephant in the area (Owen-Smith 1966). Although detailed data could not be obtained from the South African National Parks, the majority of elephant cows in the Addo Elephant Park are tuskless (Hall-Martin 1998). The incidence of tusk-

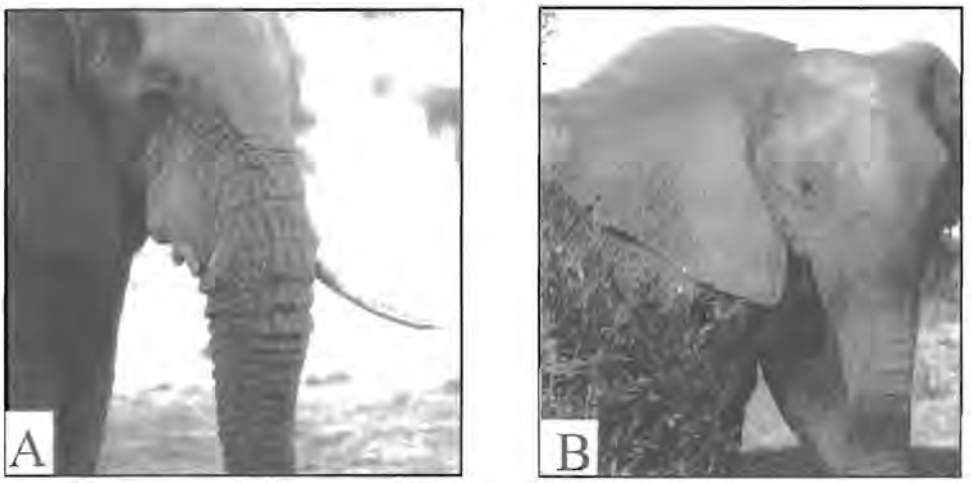

Fig. 1. The external appearances of tuskless elephant. Unilateral tusklessness (A) and bilateral tusklessness (B).

lessness amongst Asian elephant (*Elephas maximus*) is significantly higher than its African counterpart with by far the most animals being born without the capacity to grow tusks (Sikes 1971; Grzimek 1972).

This paper reports on the early development of the tush and tusk and the occurrence and anatomical considerations of tusklessness of elephant in the Kruger National Park. It furthermore proposes a theory on the role human interaction may play in selection for tusklessness in elephant breeding patterns.

Methods

Eight elephant embryos, varying in mass between 1g (less than one month gestation) and 240g (3 months gestational age) were harvested during the population control programme of the Kruger National Park (De Vos 1983). The heads of all but the smallest were hemisected, radiographed, fixed in buffered formalin and processed for routine light microscopy. The heads of all except the smallest embryo (1 g) was hemisected. Serial sections were prepared of each in the sagittal plane and stained with haematoxylin and eosin. The developmental chronology of the lamina dentalis and the primordial of the tush and tusk were recorded through microscopic examination.

Statistics were obtained during the 1990-1993 elephant population control programme of the Kruger National Park (De Vos 1983). The culling programme was carried out on a random basis and across the whole territory of the park. Results were analysed with particular reference to the occurrence of bilateral- and unilateral absence of tusks in adult

Table 1
Distribution of bilateral- and unilateral tusklessness amongst elephant bulls and cows

	Bilateral	Unilateral	
		Left	Right
Bull (n = 229)	2(0.87%)	2(0.87%)	4(1.75%)
Cow (n = 409)	17(4.16%)	6(1.46%)	15(3.67%)

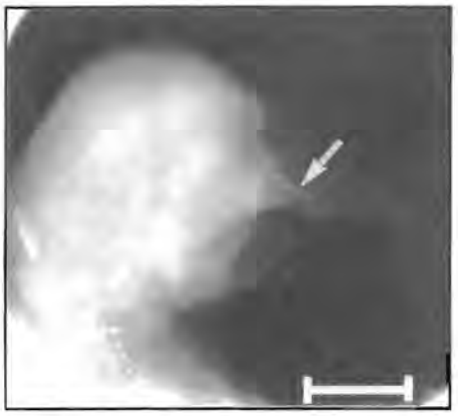

Fig. 2. Os incisivum of a 136-g embryo (arrow) showing a central radiolucent area where the development of the tush and tusk takes place (Bar = 2 cm).

Fig. 3. The early development of the dental lamina (white arrow) in the stomodeum of the 6.5-g embryo. Note the developing tongue (T), lip (L) and trunk (Tr) (H&E stain, magnification x80).

elephant (Figs. 1A & B). The maxillae of four embryos and four foetuses varying in gestational ages from 2-22 months were obtained for radiographic examination, dissection and microscopical examination. The tusked status of the maternal animals of four embryos and two foetuses were known.

Results

The earliest stage at which it was possible to identify the os incisivum (the part of the nasomaxillary complex in which the tush and tusk develop) radiologically was in a 48.8 g (2 months gestational age) embryo. The os incisivum in a 136 g (2-3 month gestational age) showed a central radiolucent area where early development of the tush and tusk was taking place (Fig. 2).

Microscopic examination of the 1g embryo showed a stomodeum lined by primitive squamous epithelium. No dental development could be identified with serial sectioning. Early development of a dental lamina was evident in the 6.5 g (1 month) embryo (Fig. 3) and the formation of the cap stage of the dental organ of the tush was evident in sections of the 48-g embryo. The dental lamina was partially intact at this stage and ectomesenchymal aggregates formed the dental follicle and dental papilla. Formation of bone was present around the dental organ (Fig. 4). A 94-g embryo showed loss of continuity of the dental lamina and maturation towards the bell stage of the dental organ of the tush was evident in sections of the 136-g embryo. At this

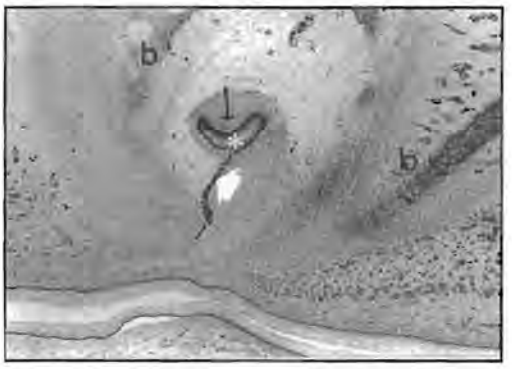

Fig. 4. The dental follicle (asterisk) and dental papilla (black arrow) of the cap stage of the dental organ of the 48-g embryo. Note the partially intact dental lamina (white arrow). Formation of bone around the dental follicle is evident (b) (H&E stain, magnification x180).

Fig. 5. Formation of the bud stage of the tusk (arrow) from the external epithelial layer of the dental organ of the tush (H&E stain, magnification x100). Inset: High magnification of the bud of the tusk (H&E stain, magnification x250).

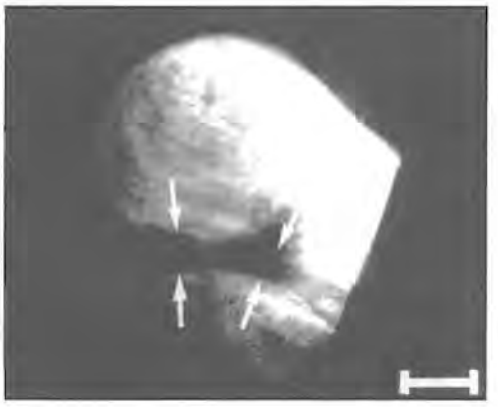

Fig. 7. Lateral radiographic view showing complete absence of tush and tusk (arrows) in the premaxilla of a 59 kg foetus. (Bar = 5 cm).

stage, epithelial proliferation of the external enamel epithelium of the bell stage of the tush formed the bud stage of the succesional tooth germ, the tusk (Fig. 5).

Of the 638 elephant (409 cows and 229 bulls) culled between 1990 and 1993, 46 (38 females and eight males) showed either unilateral or bilateral absence of tusks (Table 1). Bilateral absence of tusks affected 19 elephant (or 3 % of the total) and the frequency thereof was higher in cows than bulls (17:2). This difference was statistically significant when evaluated with the Chi-square test with Yates correction ($P = 0.03$). Although development of the tush and tusk was recorded in the majority of embryos and foetuses either microscopically or radiographically (Fig. 6),

Fig. 6. Radiograph showing normal development of the tush (arrow) and tusk (X) in the premaxilla of the 53 kg foetus. (Bar = 5 cm).

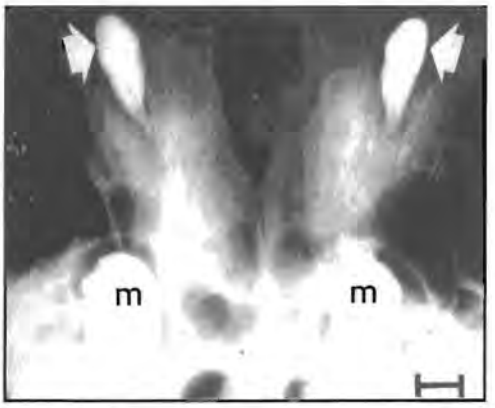

Fig. 8. Occlusal radiograph of the premaxilla of the 90 kg foetus showing the presence of both tushes only (arrows). Note the absence of tusk development between the developing molars ('m') and the tushes. (Bar = 5 cm).

one foetus showed complete absence of both the tush and tusk (Fig. 7) and another the presence of a tush only (Fig. 8). Unilateral absence of a tush or tusk was not seen in any of the embryos or foetuses examined (Table 2).

Discussion

This study has shown that the tush and tusk of the African elephant develop in succession and have a deciduous to permanent relationship. These findings are contrary to those of Anthony(1933) and Tassy (1987) who proposed the tush and tusk to represent separate teeth of the same series of incisors. This observation is supported by the radiograph in which the tush is demonstrated to lie anterior to the developing tusk. After completion of development the tush frequently fails to erupt, is pushed aside by the growing tusk and eventually resorbed in the connective tissue surrounding the os incisivum. The displacement of the tush by the growing tusk, which is clearly evident in dissected specimen of newly born elephant calves (Raubenheimer *et al.* 1994), may have prompted Anthony's observation that the tush develops adjacent to and separate from the tusk. Although the tush seems to be a non-functional vestigial dental structure, it plays an important role in the development of the tusk. The primordium of the tush not only provides the epithelial anlage for the development of the tusk, but also orientates the enamel organ of the tusk in the os incisivum and creates a pathway for the eruption thereof. Furthermore it delays the onset of the development of the tusk by several months during the first trimester of pregnancy. This delay may be important in retarding the eruption of the tusk until well after birth, thereby facilitating breast-feeding during the first year of life.

Absence of both tusks is generally congenital and may follow an inherited pattern. The occurrence of bilateral tusklessness is significantly higher in females (4.16 %) than males (0.89 %) in the Kruger National Park. Tusklessness in this sanctuary, where no selection through hunting has taken place and breeding herds remain intact, probably represents a natural mutation, which appears to be sex linked. Random culling in the Kruger National Park has contributed to this reserve becoming known for its large ivory bearing elephant (Hall-Martin 1981; Hall-Martin 1982), a sight which has disappeared from most of the African continent (Ottichilo 1986; Pilgram & Western 1986). The approach towards hunting within the ecological boundaries of the Kruger National Park

Table 2
Status of tush and tusk development in elephant embryos and foetuses

Mass	Gestational age (mnths)	Tush	Tusk	Maternal status
1 g	< 1	unknown[a]	unknown[a]	tusks L&R
6.5 g	1	L&R	unknown[a]	tusks L&R
48.4 g	2	L&R	unknown[a]	tuskless L&R
107 g	2-3	L&R	unknown[a]	tusks L&R
53 kg	17	L&R	L&R	unknown
59 kg	18	absent L&R	absent L&R	tusk L only
90 kg	21	L&R	absent L&R	unknown
94 kg	21	L&R	L&R	L&R

[a] The stage of embryonal development is to early to determine the presence of tush and/ or tusk.

seems to be changing. A hunting concession was recently granted to a neighbouring community in exchange for an agreement not to settle in an ecologically sensitive part of the park that was handed back after a successful land claim (Steyn 2000). Although limited in extent, this concession may hold consequences for future negotiations on the right to hunt in the Kruger National Park.

Individual animals in a tusked herd may become tuskless in later life as a result of injury or disease (Sikes 1971). This occurrence could be designated as acquired tusklessness and is usually unilateral with normal tusk development on the unaffected side. Unilateral tusklessness could however also be congenital resulting from failure of embryological development of the tusk on one side only. Radiographic examination, dissection and a thorough family history are essential in distinguishing unilateral acquired- from unilateral congenital tusklessness. The right-sided absence of a tusk in a cow in our study is probably genetically linked as her foetus failed to develop tushes and tusks on both sides. The 27 elephant with unilateral tusklessness were not examined thoroughly enough to distinguish the congenital from the acquired type. The higher frequency of right sided tusklessness may be indicative of tusk breakage being the most important cause for the absence of a tusk, as elephant are generally right tusked (Sikes 1971).

The involvement of the tush in tuskless elephant has not yet been recorded. Congenital absence of both the tush and the tusk imply failure to develop a lamina dentalis during the first month gestation. The presence of a tush only indicate arrest of development of the primordium of the tusk wich takes place during the second month of gestation. Tusklessness with or without tushlessness will be indistinguishable with external examination only as the tush of elephant does not appear to erupt and is pushed aside into the surrounding tissue by the growing tusk (Raubenheimer *et al.* 1994).

In order to compare the occurrence of tusklessness in the Kruger National Park with those in other elephant sanctuaries, the unilateral absence of tusks in our study was not be taken into account as in most reports only bilateral tusklessness is recorded. This study has shown that the incidence of bilateral tusklessness varies significantly between different regions. Three percent of our total sample suffered bilateral tusklessness compared to 10 % in Mana Pools. The reasons for the more frequent occurrence of tusklessness in Mana Pools when compared with the Kruger National Park are speculative. An explanation for this can possibly be found in the different population control measures employed in the two regions. In the Kruger National Park, culling has been performed randomly (De Vos 1983) and there is no chance of selection of any kind. The Kruger National Park is fenced and illegal hunting is generally under control. The elephant population in Mana Pools is managed through hunting concessions. The area is not fenced and the elephant population is exposed illegal ivory harvesting. Elephant in the Eastern Cape Province of South Africa reached virtual extinction by 1931 when only 11 survived the onslaught of ivory hunters in the dense Addo bush. Most of these elephant were tuskless. The selection for the tuskless gene is presently, 60 years after hunting was prohibited and the region declared a national park still evident, as most of the cows in the present population of 272 elephant are tuskless (Hall-Martin 1998). The shift towards tusklessness is significantly more pronounced in the elephant populations of Asia (Elder 1970; Pilgram & Western 1986) that has been exposed to modern man – hunter for much longer than its African counterpart. Most Asian elephant cows fail to develop tusks (Sikes 1971) whereas the incidence of tusklessness amongst Asian elephant bulls is much higher than on the African continent. Only 10 % of elephant bulls in Sri Lanka are reported to have tusks (Grzimek 1972). Three thousand years of exposure to man who hunted for ivory and domesticated elephant to perform work, thereby disrupting hierarchal order and breeding patterns,

selected for a phenotype, which generally lacks the genetic capacity to develop ivory tusks.

The modern high velocity rifle no longer respects and in fact selects the large tusk bearing elephant as its contribution to the population control programmes of areas managed through hunting concessions. The undisputed illegal ivory harvesting by those who frequently use armour piercing weaponry in immobilising a large tusker, contribute significantly to the heavy demand placed on the already compromised genetic pool of large tusk carriers. This is in contrast to the methods of hunting employed before the arrival of technology to the African continent. During most of the 19th century and even in the early 20th century elephant hunting and trapping methods like the falling spear, the wheel trap, trunk snare, hamstring and tendon slashing as well as group hunting with heavy short shafted spears (Sikes 1971) were more successful in killing smaller and weaker animals and in fact probably contributed positively towards the selection for a larger tusked phenotype. The arrival of the modern weapons in Africa coincided with the rapid disappearance of large tusk bearing elephant (Sikes 1971; Ottichilo 1986). Although elephant with tusks weighing in access of 80 kg was a common sight in the past century, elephant herds in most areas now consist of small-tusked animals only. Over a long period, this selection will not only lead to a decrease in the large tusked population, but also a relative increase in tuskless animals due to the hunters' lack of interest in elephant without tusks. The trend towards bilateral tusklessness is even higher in the sub adult elephant population in Mana Pools (Owen-Smith 1966), implying that a genetic shift towards tusklessness may have taken place amongst younger animals in certain regions. These changes can possibly be explained by the dominant role the matriarch (usually the cow with the largest tusks - Sikes 1971) play in selecting cows for breeding within her breeding herd. If she is shot (her large tusks usually make her the animal of choice during both trophy hunting and illegal ivory harvesting) a breakdown of the hierarchy within her breeding herd could result in cows of lesser status (i.e., those without tusks) entering the reproductive cycle. Once the genetic balance has swung in favour of tusklessness, a return to normal hierarchical order may not be sufficient to re-establish the ivory bearing genome. This is clearly witnessed in the present day Asian elephant population.

Monitoring of the size of tusks as well as the incidence of bilateral tusklessness are important indicators for genetic selection in nature conservation areas. Randomised population control programmes should be introduced where a reduction of elephant numbers are necessary. Authorities issuing hunting concessions in Africa should take note of the trends reported in this manuscript and introduce a tariff structure, which would encourage hunting of a broader spectrum of elephant in a herd. Restoration of the matriarchal dominance in a breeding herd seems imperative to the long-term survival of the ivory bearing gene. The granting of permits for international trade in ivory should, in the long term, be based on whether a region is successful in maintaining the ivory bearing phenotype during their population control programme.

Acknowledgements

The Research Division, South African National Parks (Dr V. de Vos in particular) is thanked for supplying the data and material and Mrs C.S. Begemann for secretarial assistance. This study was supported by a grant from the National Research Foundation of South Africa.

References

ANTHONY, R. 1933. Recherche sur les incisives superieures des Elephantidea actueles et fossils. *Archives du Museé national d'Histoire naturelle. Paris* 10: 61 – 124.

DE VOS, V. 1983. Management of large animals in African conservation areas. Pp. 213-32. *In*: OWEN-SMITH, M.A. (ed.). *Proceedings of a Symposium held in Pretoria, 29 – 30 April 1982.* Pretoria: Haum.

ELDER, W. H. 1970. Morphometry of elephant tusks. *Zoologica Africana:* 143 – 59.

GRZIMEK, B. 1972. *Grzimek's Animal Life Encyclopaedia.* (Edited by GRZIMEK B.), Vol. 12. New York: Van Nostrand Reinhold.

HALL-MARTIN, A. 1981. Kruger's big tuskers. *African Wildlife* 35(1): 6–9.

HALL-MARTIN, A. 1982. Kruger's tuskers. *African Wildlife* 36(2): 69.

HALL-MARTIN, A. 1998. Addo. *Africa Environonment and Wildlife* 6(6): 66–77.

OTTICHILO, W.K. 1986. Age structure of elephants in the Tsavo National Park, Kenya. *African Journal of Ecology* 24(2): 629–75.

OWEN-SMITH, N. 1966. The incidence of tuskless elephant in Mana Pools Game Reserve. *African Wildlife* 20: 69–73.

PILGRAM, T. & D. WESTERN. 1986. Inferring the sex and age of African elephants from tusk measurements. *Biological Conservation* 36: 39–52.

RAUBENHEIMER, E.J., W.F.P. VAN HEERDEN, P.J. VAN NIEKERK, V. DE VOS & M.J. TURNER. 1994. Morphology of the deciduous tusk (tush) of the African elephant (*Loxodonta africana*). *Archives of Oral Biology* 40(6): 571–76.

SIKES, S.K. 1971. The Natural History of the African Elephant. London: Weidenfeld and Nicholson.

STEYN, T. 2000. To hunt or not to hunt in a national park. News 24.co.za, 27 January.

TASSY, P. 1987. A hypothesis on the homology of Proboscidean tusks based on paleontological data. *American Museum Novitates* 2895: 1–18.

Pergamon

0003-9969(95)00008-9

Archs oral Biol. Vol. 40, No. 6, pp. 571–576, 1995

0003-9969/95 $9.50 + 0.00

SHORT COMMUNICATION

MORPHOLOGY OF THE DECIDUOUS TUSK (TUSH) OF THE AFRICAN ELEPHANT (*LOXODONTA AFRICANA*)

E. J. RAUBENHEIMER,[1] W. F. P. VAN HEERDEN,[1] P. J. VAN NIEKERK,[1] V. DE VOS[2] and M. J. TURNER[1]

Department of [1]Oral Pathology and Oral Biology, P.O. Medunsa, 0204 and [2]Research Division, Skukuza, Kruger National Park, Republic of South Africa

(Accepted 10 January 1995)

Summary—The tusk of the African elephant is preceded by a deciduous tooth generally known as the tush. Tushes from nine elephant fetuses and six calves younger than 1 year were exposed by dissection and described morphologically. All tushes consisted of a crown, root and pulpal cavity, the formation of which is completed soon after birth. They reached a maximum length of 5 cm, appeared not to erupt through the skin and were pushed aside and resorbed during enlargement of the distally located primordium of the tusk. Dental enamel, which covered the crown, could easily be removed and consisted of rods with an interwoven arrangement; the dentine–enamel junction was flat. Cellular cementum extended for variable distances over the crown and the dentine was tubular in nature. Although the tush apparently has no function, it provides the anlage and orientation for the development of its permanent successor.

Key words: tush, African elephant, *Loxodonta africana*, deciduous tusk.

The tusk of the African elephant (*Loxodonta africana*) is a modified premaxillary lateral incisor tooth which erupts at an age of approx. 1 year (Grzimek, 1972). It is preceded by a deciduous tooth commonly referred to as the 'tush'. The tush is reported to develop in the same alveolar cavity as the tusk and may reach a length of 5 cm (Sikes, 1971). Although it is generally accepted that the tush is the deciduous precursor to the tusk, palaeontological data provide some evidence that the two teeth develop independently and that they could represent deciduous central and deciduous lateral incisors, respectively (Tassy, 1987). Our purpose now was to determine the morphology of the tush of the African elephant, *Loxodonta africana*.

The maxillae of the nine elephant fetuses and six calves younger than 1 year were obtained during the elephant population control programme of the Kruger National Park (de Vos, 1983) and fixed in buffered formalin. The specimens were examined radiographically and the tushes exposed by dissection. The relation to the developing tusk was noted and all the tushes removed. Each tush was measured and divided along its length in two halves. One half was processed for light microscopy and the other for scanning electron microscopy. Half of the samples for light microscopy were mineralized, routinely sectioned and stained with a haematoxylin and eosin; ground sections were prepared from the remainder.

All tushes were embedded in the premaxillae and located anteriorly to the primordium of the developing tusk (Fig. 1). The tush and the primordium of the tusk were in the same bony cavity. The crowns of the tushes in the older calves were visible outside the alveolar bone. None of the specimens showed a tush which had erupted through the overlying skin. A radiograph, which was taken of the tusk of a 5-year-old elephant, demonstrated the crown of a tush embedded in the soft tissue around the girth of the tusk (Fig. 2). All tushes could, by external examination, be subdivided into a crown covered by enamel and a slender root. A cervical constriction was absent and the incisal margin rounded (Fig. 3). The formation of enamel was incomplete in the incisor region of five tushes, of which two were from the same animal (Fig. 4). The longest tush measured 5 cm in length and formation of the crown appeared to be completed after 16 months of gestation. Root formation was found to be completed during the first 3 months post partum, whereafter root resorption, mediated by osteoclast-like giant cells, coincided with progressive enlargement of the distally located primordium of the tusk (Figs 5 and 6). External resorption was not only restricted to the root, but also involved the crown of the tushes.

The enamel, which covered the crown, could be removed with a sharp instrument without difficulty from the underlying dentine. It consisted of rods of 4–6 μ dia. Bundles of enamel rods followed an interwoven course to the surface of the tooth (Fig. 7). This arrangement was consistent throughout the entire enamel. The enamel–dentinal junction was flat, enamel tufts were infrequent and the dentine was of

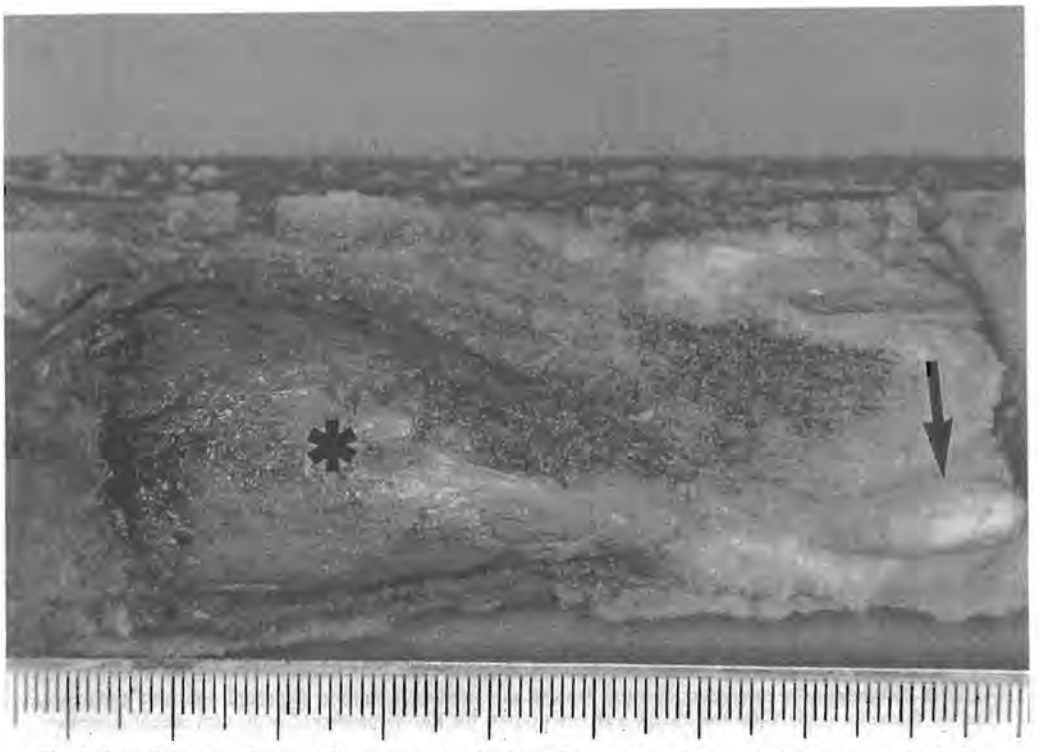

Fig. 1. Length section through the premaxilla of a fetus. The tush (→) is located anterior to the follicle of the developing tusk (*). Scale in mm.

a tubular nature. Cellular cementum covered the roots and in fully formed teeth extended over the external surface of the crown (Fig. 8).

Fig. 2. Radiographic view of the girth of the tusk of a 5-year-old elephant. Note the crown of the tush, its rounded tip pointing anteriorly, which was pushed aside and found to be located in the subcutaneous soft tissue (→). Bar = 1 cm.

The question whether the tush represents a deciduous precursor to the tusk (Sikes, 1971) or whether it is an incisor which develops independently from the tusk (Tassy, 1987) cannot be resolved in a study of this nature. Dissection of embryos at an earlier stage of development will throw more light on the initial relation between the follicles of the two teeth. In the specimens we examined the possibility of independent tush development seems unlikely as both the tush and tusk were located in one alveolar cavity, with the tush anterior to the developing tusk.

Although superficial reference has been made to the tush of the African elephant (Sikes, 1971; Grzimek, 1972), its morphology, structure and functions have never, to the best of our knowledge, been recorded. The function of this deciduous incisor is unclear because, unlike the tusk, it does not appear to make its presence visible by erupting through the skin. The pressure exerted by the growing tusk leads to resorption of the root of the tush by osteoclast-like giant cells soon after birth and it appears as if its crown is pushed aside and into the soft tissue surrounding the girth of the growing tusk. The fate of the displaced crown is speculative, although it seems likely that it is eventually completely resorbed. It may be argued that the tush represents an evolutionary remnant of a tooth that may have had a function in the earlier extinct Proboscideans, where incisor teeth had a more pronounced masticatory function (Grzimek, 1972). When viewed in an embryological context, the primordia of primary teeth provide the anlage and orientation for the development of their permanent successors (Bhaskar, 1980). This may

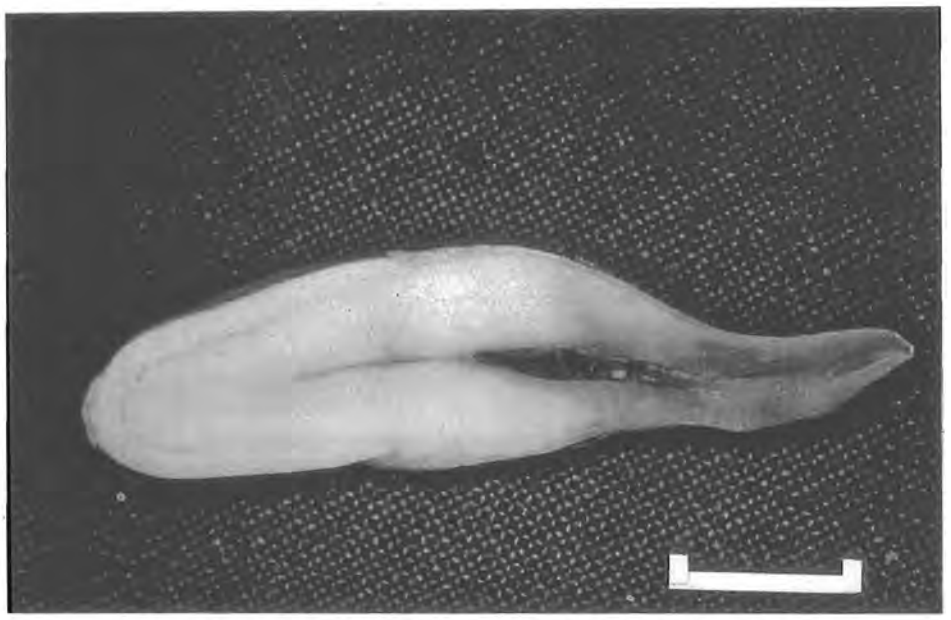

Fig. 3. Section cut in length through a fully formed tush. Bar = 1 cm.

represent the only distinct function of the tush of the African elephant.

Despite its apparent regression in the course of evolution, the tush is composed of an orderly arrangement of all tissue types found in mammalian incisors. The ease with which the enamel could be removed from the underlying dentine is explained by the flat enamel–dentinal junction. Incomplete enamel formation, involving particularly the incisal margin, appears to be a frequent occurrence. Formation of cementum on the external surface of the crown is not uncommon in the animal kingdom. In many animals, the reduced enamel epithelium breaks down long before the tooth erupts, allowing the ectomesenchyme of the tooth follicle to come into contact with the enamel. This is followed by the differentiation of cementoblasts and the deposition of coronal cementum.

The stage of dental development reflects the age of fetuses and infants. Although a limited number of

Fig. 4. A dissected specimen in which the skin and soft tissue of the premaxilla had been removed, thereby partially exposing the crown of a tush, which is viewed from the anterior. Note the area of deficient enamel formation (→). Bar = 2 cm.

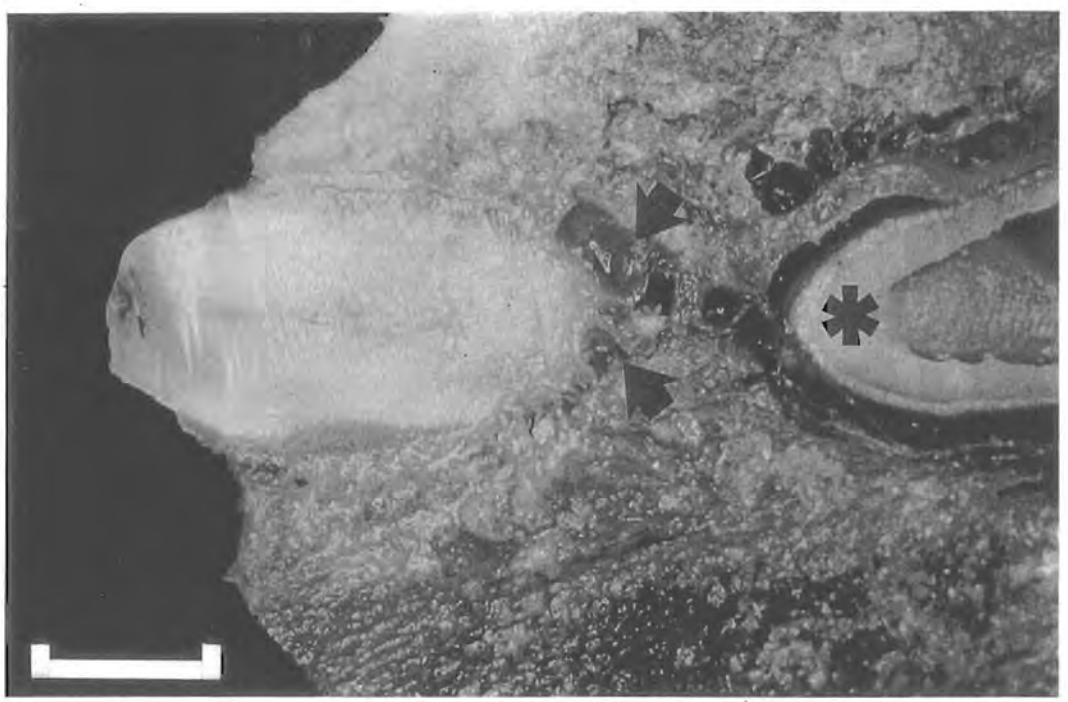

Fig. 5. Longitudinal section through tush of a newborn calf, which has erupted through the cortical plate of the alveolar bone. Note the proximity of the tip of the enlarging tusk (*) and its association with resorption of the root of the tush (→). Bar = 1.6 cm.

elephants have been examined, it appears as if the crown of the tush is completed by the 16th month of intrauterine life and root development ceases 3 months after birth, which follows after 22 months' gestation (Sikes, 1971). After formation of the tush has been completed, the enlarging primordium of the tusk displaces it and resorption commences before the postnatal age of 1 year.

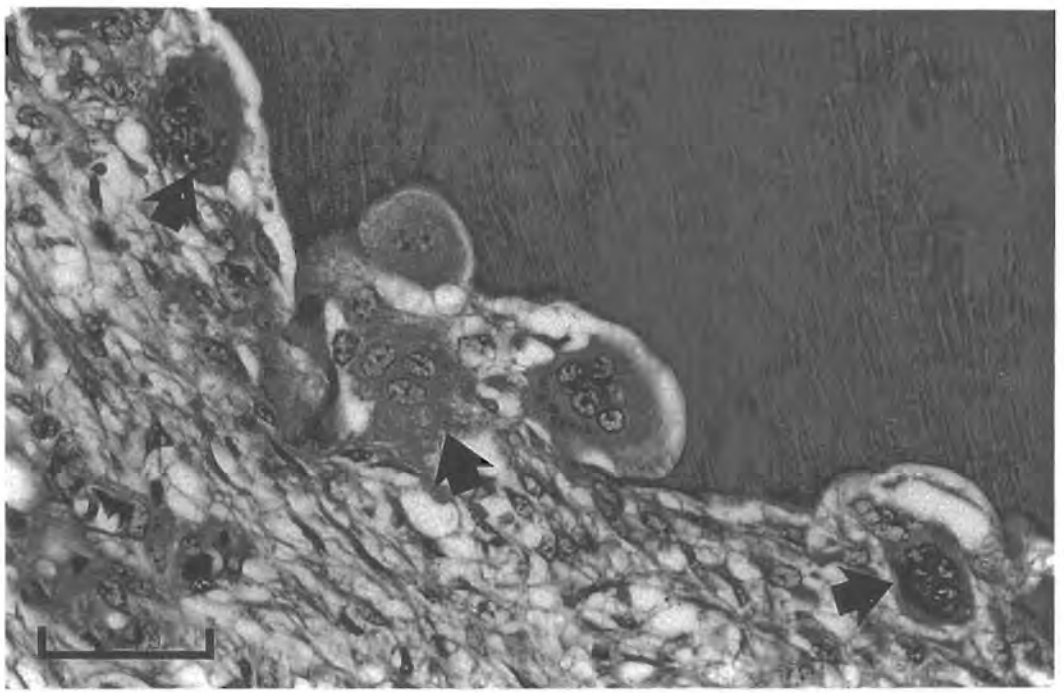

Fig. 6. Photomicrograph showing active resorption of the dentine of the root of a tush by multinucleated giant cells (→). H & E, ×400; bar = 50 μm.

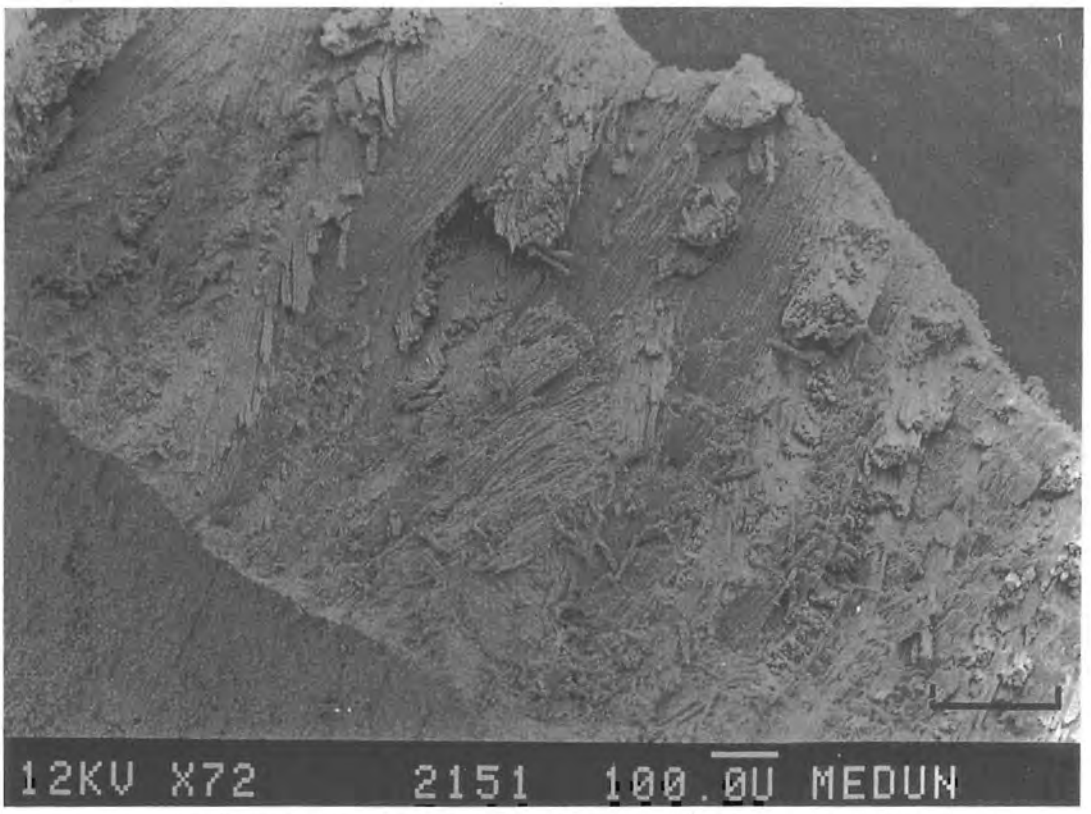

Fig. 7. Scanning electron micrograph of a fracture surface of enamel (bottom left—dentinal junction, top right—outer surface). ×72; bar = 200 μm.

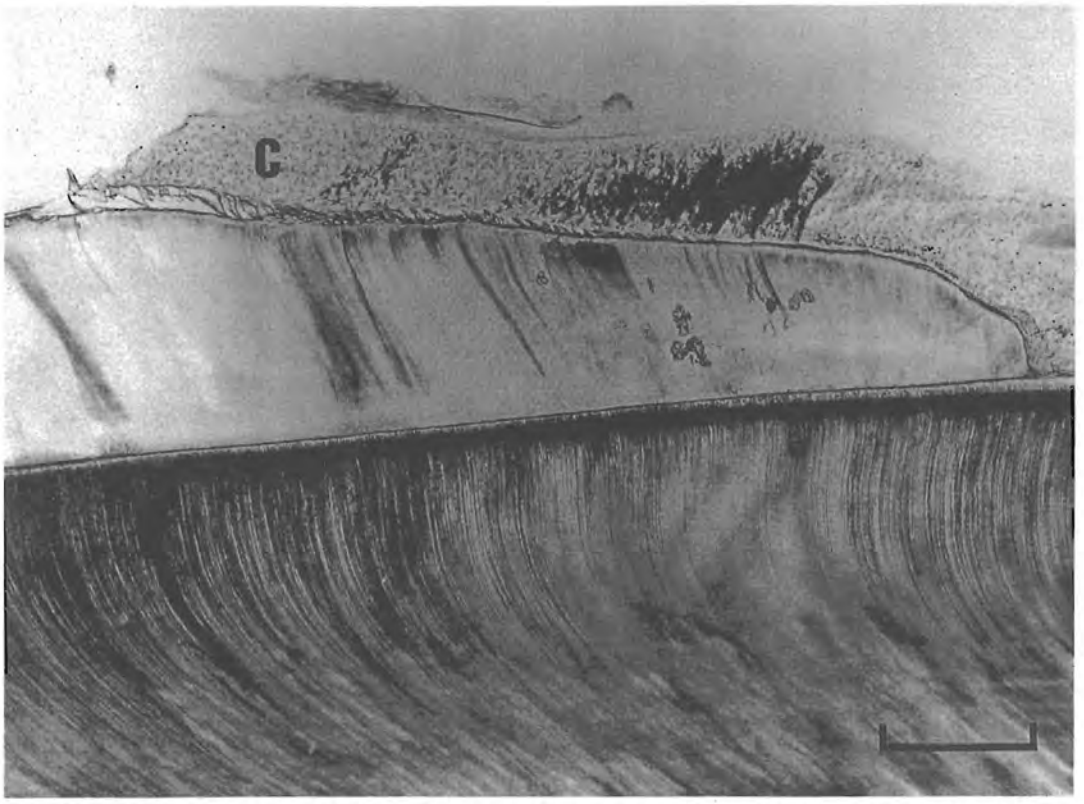

Fig. 8. Cellular cementum (C) extending on to the external surface of the crown. Note the flat dentine–enamel junction. Ground section, ×20; bar = 1 mm.

REFERENCES

Bhaskar S. N. (1980) *Orban's Oral Histology and Embryology*, Chap. 2, pp. 24–45. The C. V. Mosby Company, St Louis.

Grzimek B. (1972) *Grzimek's Animal Life Encyclopedia*, Vol. 12, p. 479. Van Nostrand Reinhold, New York.

Sikes S. K. (1971) *The Natural History of the African Elephant*, Part 1, pp. 81–82. Weidenfeld and Nicholson, London.

Tassy P. (1987) A hypothesis on the homology of Proboscidean tusks based on paleontological data. American Museum Novitates 2895, 4th November, 1–18.

de Vos V. (1983) Management of large animals in African conservation areas. *In Proceedings of a Symposium held in Pretoria 29–30 April 1982.* (Ed. Owen-Smith M. A.), pp. 213–232. Haum, Pretoria.

Morphological aspects and composition of African elephant (*Loxodonta africana*) ivory

E.J. RAUBENHEIMER

Raubenheimer, E.J. 1999. Morphological aspect and composition of African elephant (*Loxodonta africana*) ivory. *Koedoe* 42(2): 57–64. Pretoria. ISSN 0075-6458.

This study was aimed at determining the origin of the diamond shaped pattern and composition of ivory of the African elephant. Fragments of ivory and tusks were obtained through the National Parks Board from the Kruger Park, Addo Elephant Park, Kaokoveld, Caprivi, Etosha, Kavango and Tembe Elephant Park. Polished surfaces were prepared in different planes and examined with light and electron microscopical techniques. Analyses of the inorganic composition were performed using atomic absorption spectrophotometry, ion selective electrodes and inductively coupled optical emission spectroscopy. The total amino acid composition was determined with the aid of an amino acid analyser. Morphological investigations showed the distinctive diamond shaped pattern of ivory to be caused by the sinusoidal surface to pulpal course followed by odontoblastic tubules. This course is the result of pressure which builds up between tightly packed odontoblasts on their centripetal course along an ever decreasing pulpal circumference during formation of ivory. A total of 17 elements were detected in the inorganic fraction of ivory, some in concentrations as low as 0.25 µg/g. The concentrations of calcium, magnesium, fluoride, cobalt and zinc showed statistically significant differences ($P < 0.007$) between selected regions and may prove valuable in distinguishing chemically between ivory from different geographical locations. The organic content of ivory showed 17 amino acids in varying concentrations. The possible causes of these variations are discussed.

Key words: elephant ivory, morphology, composition

E.J. Raubenheimer, Department of Oral Pathology, MEDUNSA, P.O. Medunsa, 0204 Republic of South Africa (ejraub@mcd4330.medunsa.ac.za).

Introduction

The paired tusks of the African elephant are incisors which develop in the os incisivum of the nasomaxillary complex of bones and which grow continuously throughout life. The unique diamond shaped pattern of elephant ivory, which has not been researched in great detail (Sognnaes 1960; Miles & Boyde 1961; Sikes 1971; Raubenheimer *et al.* 1990) has made it a sought-after product in the manufacturing of works of art. The flourishing illegal trade in ivory has contributed to a significant decrease in elephant numbers on the African continent over the past decades (Armstrong & Bridgland 1989). The Convention on International Trade in Endangered Species (CITES) at its biennial meeting in Lausanne, Switzerland in October 1989 responded by placing a ban on the trade in elephant products. The effect of this ban on well managed elephant populations in Southern African states remains controversial.

Dentine (or ivory) forms the bulk of most teeth and is composed of organic and inorganic fractions. The inorganic composition of elephant ivory has not yet been investigated in detail except for distinguished work done on its carbon and nitrogen isotope ratios. The carbon isotope ratios ($^{13}C:^{12}C$) of ivory distinguishes between elephant roaming woodland and those in dense forests (Van der Merwe *et al.* 1990). The aims of this study were to determine the origin of the chequered (diamond shaped) pattern of elephant ivory and establish a databank on the inorganic and organic composition of ivory from the Southern African region.

Material and methods

Twenty fragments of ivory and five tusks, with masses between 0.7 and 9.3 kg were sectioned and polished in cross sections and sagittal planes and the characteristic diamond shaped pattern studied. One developing tusk was harvested from a full-time fetus 20 minutes after death. Biopsies were taken from the pulpal ivory and soft tissue, cut in thin slices and fixed in 10 % phosphate buffered formalin. Ground sections, 40 µ thick were prepared parallel and perpendicular to the long axis of 12 different fragments of ivory and subjected to light microscopic examination. Routine techniques for the preparation of scanning electron micrographs of hard tissue were employed to visualise the morphology and distribution of dentinal tubules of six different tusks. An image analyser (FIPS, CSIR, Pretoria) was used to measure the distances between the tubules in the light and dark bands respectively.

Sixty four fragments of ivory were obtained through the South African National Parks from Kaokoveld, Etosha National Park, Caprivi, Kavango, Kruger National Park, Tembe Elephant Park and Addo Elephant Park. Specimens weighing between 0.5 g and 1.0 g were prepared by removing the ensheathing layer of cementum with a rotating diamond disc. The specimens were agitated in a weak acid (0.1M HCl) for 10 minutes to remove all traces of metal that may have contaminated the ivory during sample preparation. The fragments were washed for 15 minutes in distilled water and the dry weights of each fragment determined accurately. Each specimen was completely demineralised in 1M perchloric acid. The inorganic composition was determined by atomic absorption spectrophotometry (Perkin Elmer 500; Norwalk, CT, U.S.A.), Astra 8 analyser (Beckman Instruments Inc., Brea, CA, U.S.A.) and ion selective electrodes (Radiometer, Copenhagen, Denmark). The mean values obtained per site of origin as well as the standard deviations (SDs) were expressed in mg/g dry weight and tabulated. The level of significance between the concentrations of each element at different geographical sites was determined with the Student *t*-test for unequal variances. The trace elemental composition of 25 fragments was determined with an inductively coupled plasma optical emission spectroscope (ARL 3400, Boston, MA, U.S.A.). Perchloric acid (1M) was used as a control. The mean concentrations and SDs were expressed in µg/g ivory.

Samples of ivory, weighing between one and three grams, were prepared from 32 fragments of ivory obtained from Kruger National Park (5), Kaokoveld (6), Etosha (15), Tembe (4), and Addo Elephant National Park (2). The samples were hydrolysed in sealed tubes containing 5 ml 6M HCl at 110 °C for 24 hours. The hydrolysates were neutralised, filtered (Millex-GS, 0.22 µ) and diluted 1:1 with citrate buffer (pH 2.2). Calibrants of 43 amino acids were prepared and the amino acid composition of the hydrolysate and calibrants determined using a Beckman 6300 Amino Acid Analyser. The chromatograms were integrated and quantified using a Hewlett-Packard 3390A integrator. The results were tabled as the average of the residues per 100 and the standard deviation for each amino acid calculated.

Results

The pulpal cavity of the tusks were conical in shape, had a smooth surface and a large pulpal opening. The bulk of a large tusk consisted of ivory (Fig. 1a). The entire outer

Fig. 1a. Partially dissected tusk exposing the conical pulpal cavity, diamond-shaped pattern (exposed on a polished surface prepared on a cross section) and parallel and alternating light and dark lines (on polished surface prepared in the sagittal plane). Note the large apical opening of the pulp on the left and the solid ivory forming the bulk of the tip of the tusk.

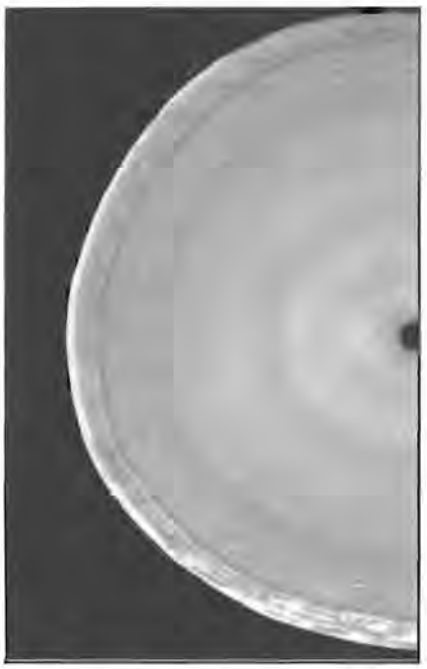

Fig. 1b. Closer view of the diamond-shaped pattern on cross section through the tusk. Note the ensheathing layer of cementum and scalloped ivory to cementum junction.

Fig. 1c. Closer view of the sagittal surface showing the alternating dark and light lines.

surfaces of the tusks were found to be covered by a layer of cellular cementum. The cementum to ivory junction was visible as a dark concentric ring. In cross sections, the ivory to cementum junction followed an undulating circular course, forming irregular excrescences alternating with shallow convexities or concavities (Fig. 1b). In this plane, the unique diamond-shaped pattern of the ivory consisted of two systems of alternating light and dark lines which radiate clockwise and anticlockwise, respectively, from the axis of the tusk. The diamond-shaped pattern corresponded to parallel light and dark lines evident on polished surfaces prepared in the sagittal plane (Fig. 1c). The external surface of the tusk followed the contour of the cementum to ivory junction, resulting in parallel longitudinal ridges and troughs which were visible upon external examination of a tusk.

The outermost layer of ivory (mantle layer) consisted of irregularly-spaced odontoblastic tubules which slanted apically and branched extensively. When followed towards the axis of the tusk, the tubules became more evenly spaced and gradually changed their course by curving towards the tip of the tusk. This curvature was found to be the beginning of the regular, sinusoidal course followed by the odontoblastic tubules in a pulpal direction and was present only in sections prepared in the sagittal plane. The convexities and concavities of the sinusoidal pattern corresponded to the alternating light and dark bands seen macroscopically on surfaces prepared in the sagittal plane. The dark bands corresponded with that part of the tubule that curved towards the pulpal opening (Fig. 2a). On high power maginification many dentinal tubules appeared to end blind and others fused, forming one tubule (Fig. 2b). The process of fusion was distinct from the fine lateral branches that seemed to anastomose with those of adjacent tubules. Blind ending tubuli occured more frequently in the dark bands (16 blind ending tubules per 100 tubules, SD 7) than in the light bands (6 blind ending tubules per 100 tubules, SD 3) as counted over 2 500 tubules in each of the bands respectively. Microscopic sections of biopsies of the foetal tusk confirmed the distal slant of the odontoblasts and scattered pyknotic cells, highly suggestive of individual cell death (Fig. 3).

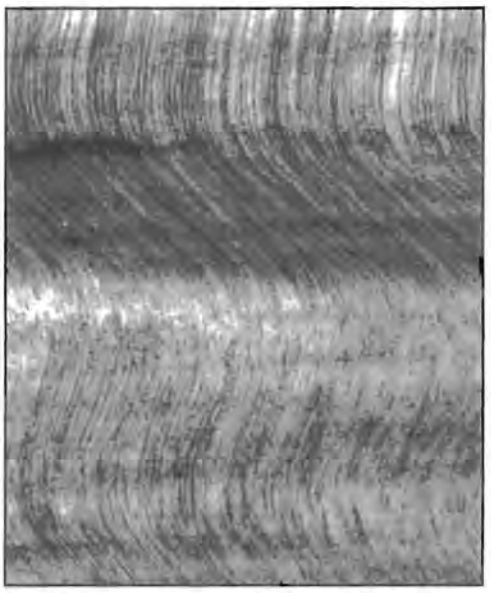

Fig. 2a. The regular sinusoidal curve followed by the odontoblastic tubules. The curve to the right coincides with a dark band (top of figure), an optical phenomenon caused by the increased density of tubules in this region. The tip of the tusk is towards the left. (Unstained section, magnification x180).

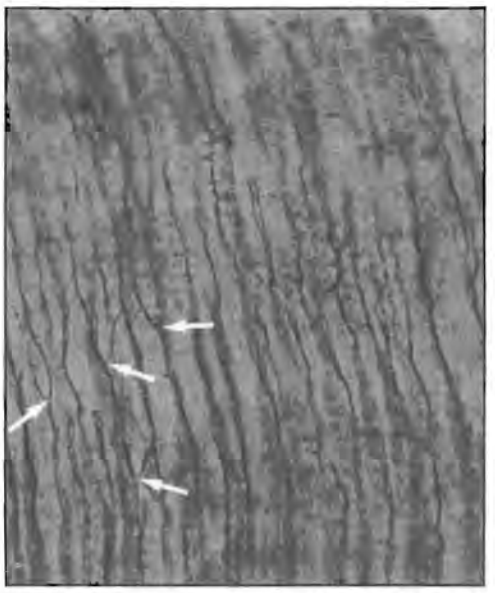

Fig. 2b. Higher power magnification in a dark band, showing fusion of tubles (arrows) (Unstained section, magnification x400).

Scanning electron microscopy showed the pulpal openings of tubules to be oval, with the greatest dimension parallel to the long axis of the tusk (Figs. 4a & 4b). Dentinal tubules were closer packed in areas where they curve towards the pupal opening (i.e. dark bands) (mean distance 4.6 ± 1.7 µm SD) than in the part of the tubule that curves towards the tip of the tusk (i.e. light bands) (mean distance 7.2 ± 2.8 µm SD) (Fig. 2a). This difference was significant ($P < 0.001$). The number of tubules/mm² varied between 31.6 x 103 and 54.3 x 103.

The inorganic composition of ivory is reflected in Table 1. Statistical analyses showed the differences between the respec-

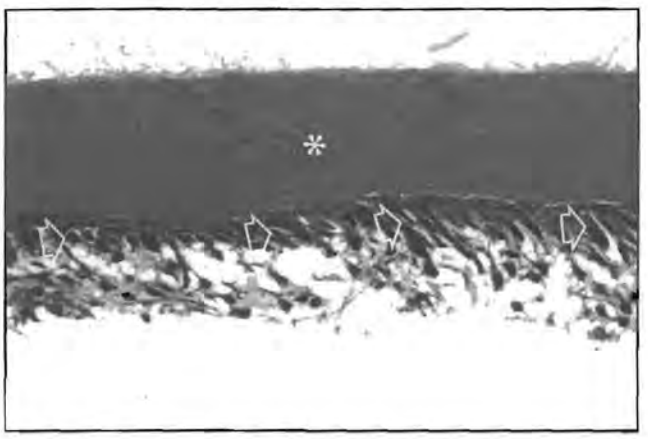

Fig. 3. Microscopic appearance of the foetal tusk. Note the newly formed ivory (asterisk) slanting of the odontoblasts and occasional cells exhibiting cell death (arrows) (H&E stain, magnification x250).

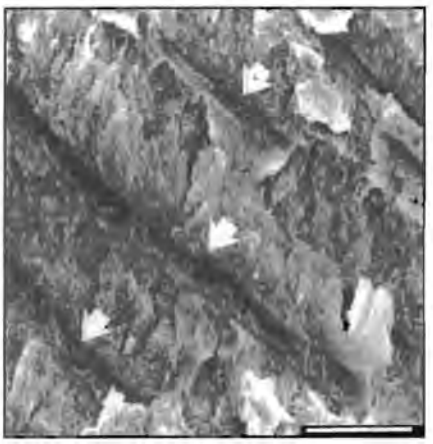

Fig. 4a. Electron micrograph of a fractured surface of ivory. Note the exposed odontogenic tubuli (arrows) (bar = 10 µm).

Fig. 4b. High power magnification of the pulpal opening of an odontoblastic tubule (bar = 1 µm).

tive elements in the following geographical locations were highly significant ($P < 0.002$):

Calcium: Addo vs. all other locations, Etosha vs. Caprivi, Etosha vs. Kavango and Caprivi vs. Tembe.

Phosphate: Kruger Park vs. Kaokoveld, Addo vs. Kaokoveld.

Magnesium: Addo vs. Kruger Park, Caprivi and Tembe vs. Addo and Kaokoveld vs. Caprivi.

Fluoride: Kaokoveld vs. all locations except Etosha and Etosha vs. all locations except Kaokoveld.

The following trace elements were detected in ivory (average content expressed in µg/g dry weight, SD in brackets: As:8.0 (1.4), Cd:0.4 (0.04), Cr:3.7 (0.6), Co:0.72 (0.09), Cu:2.2 (1.2), Pb:8.7 (1.2), Mn:0.9 (0.6), Hg:1.4 (0.2), Ni:0.89 (0.1), Zn:20 (10.8), Mo:0.56 (0.06) and Al:6.2 (4.3).

Table 1
Main inorganic elements in ivory, expressed per site of origin (average mg/g dry weight, SD in brackets)

	KNP[1]	Kaoko[2]	Etosha	Caprivi	Kavango	Tembe	Addo
No. of Specimens	13	9	26	6	4	3	3
Ca	195.8 (17)	193.7 (15.9)	192 (16)	208.9 (6.4)	205.9 (1.8)	191.1 (8.9)	170.8 (2.5)
PO_4	115.5 (5)	118 (2.6)	116 (3.5)	114.7 (4)	115.3 (3)	113.1 (5)	113 (1.4)
Mg	14.6 (3.2)	18.2 (4.2)	15.3 (4.2)	13.1 (0.9)	12.2 (2.7)	14.7 (1.2)	17.3 (0.4)
F	0.076 (0.014)	0.106 (0.017)	0.124 (0.029)	0.069 (0.012)	0.058 (0.01)	0.054 (0.009)	0.035 (0.019)

[1] Kruger National Park
[2] Kaokoveld

Ivory obtained from the Kaokoveld was more brittle and hydrolysed more rapidly than those from other regions. The amino acid composition of hydrolysed ivory is expressed in Table 2. The difference in the hydroxylysine content between Kruger and Northern Namibian ivory (Kaokoveld and Etosha) was significant ($P < 0.01$) (Kruger ivory 0.7 ppm, SD 0.1; Etosha 0.4 ppm, SD 0.1; Kaokoveld 0.4 ppm, SD 0.2).

Discussion

The cell responsible for the formation of ivory (or dentine) is the odontoblast. Odontoblasts are derived from the mesenchyme of the dental pulp and after differentiation they move centripetally (i.e. towards the axis of the tusk) and deposit ivory along their pathway. Each odontoblast is responsible for the formation of a cytoplasmic extension. Mineralisation of ivory around this extension forms tubules which traverse the diameter of the ivory. The microporosity of ivory, which is well beyond the resolution of the human eye, is responsible for the absorbent and tactile characteristics thereof, which has made it an unequalled product for the manufacturing of piano keys.

Table 2
Total aminoacid composition of 32 samples of hydrolysed ivory

Aminoacid	Residues/100	(SD)
Aspartic acid	5.1	(0.3)
Hydroxyproline	9.9	(1.0)
Threonine	2.0	(0.2)
Serine	4.0	(0.2)
Glutamine	8.0	(1.3)
Proline	12.2	(1.2)
Glycine	30.8	(1.0)
Alanine	10	(1.2)
Valine	2.3	(0.3)
Methionine	0.4	(0.4)
Isoleucine	1.2	(0.1)
Leucine	3.0	(0.1)
Phenylalanine	1.5	(0.1)
Hydroxylysine	0.4	(0.2)
Lysine	2.7	(0.7)
Histamine	0.7	(0.2)
Arginine	4.6	(0.4)

The tip of the concial pulp becomes solid as ivory depositioning progresses and lengthening of the proximal edge coincides with forward movement and elongation of the tusk.

The centripetal movement of odontoblasts during the formation of ivory leads to a rapid decline in the pulpal circumference. As a result, odontoblasts become progressively more tightly packed and intercellular pressure increases as the pulpal circumference becomes smaller. Morphological manifestations of the increased pressure between odontoblasts are reflected as a significant reduction in the distance between odontoblastic tubules in the dark bands, the oval shape of the tubules as well as the slanting of odontoblastic cell bodies towards the pulpal opening. The only means by which the growing pressure between the centripetally moving odontoblasts on a rapidly decreasing perimeter can be accommodated, is through two processes namely, movement of the odontoblastic cell mass towards the pulpal opening or a reduction in the number of odontoblasts. There is morphologic evidence that both these phenomena occur during the formation of ivory. Movement of the odontoblastic cell bodies towards the pulpal opening coincide with the dark bands (i.e. slanting of the sinusoidal curve of the odontoblastic tubuli towards the pulpal opening). As pressure increases, the number of odontoblasts are reduced through fusion of cells (represented by fusing tubules) and cell death (represented by blind-ending tubules). The occurance of the latter phenomenon is supported by the presence of pyknotic odontoblasts seen in microscopic sections of the rapidly fixed biopsies of the foetal tusk. The relief of intercellular pressure through these mechanisms results in a change in the direction of odontoblastic movement towards the tip of the tusk. This coincides with the anteriorly directed part of the sinusoidal curve. The process of odontoblastic crowding, followed by a bodily movement of odontoblasts towards the pulpal opening and a relief of intercellular pressure through cell fusion and death, with subsequent change in the direction of movement of the cell bodies are probably responsible for the regular sinusoidal

course followed by odontoblasts. This hypothesis is reflected graphically in Fig. 5. The sinusoidal course of the tubules in ivory is reflected as parallel and alternating light and dark bands which are seen on polished surfaces prepared along the axis of the tusk. The light and dark bands were found to be the result of the varying compactness of dentinal tubules between the sectors of the sinusoidal curve of the tubules that slant towards the tip of the tusk or towards the pulpal opening respectively. On cross sections, the diamond-shaped pattern is a reflection of the alternating light and dark bands seen on surfaces prepared in length. This implies that when the layer of odontoblasts are viewed in a radial perspective, movement of odontoblasts towards the pulpal opening with curving of odontoblastic tubules does not occur at the same time but rather as a wave that spreads circumferentially along the peripulpal layer of odontoblasts. On microscopic examination, it was observed that fractures through ivory generally follow the dark bands. The higher number of tubules per unit area probably makes the dark bands weaker than the light bands.

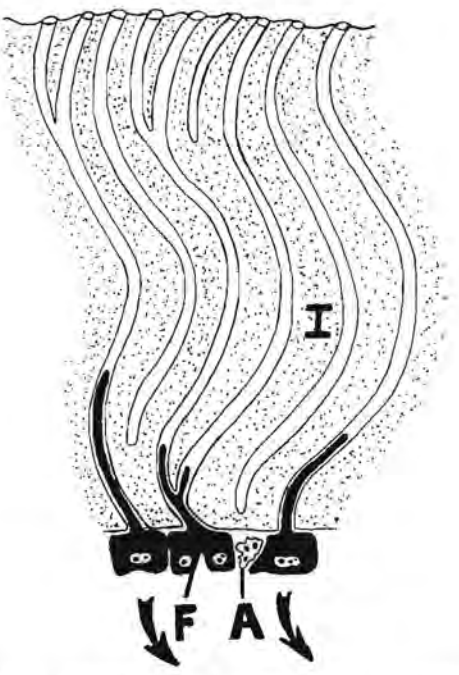

Fig. 5. Schematic representation of the sinusoidal course followed by the odontoblastic tubules (sagittal plane, the tip of the tusk is towards the right, surface towards the top and pulpal cavity towards the bottom of the figure). Note odontoblastic fusion (F) which results in odontoblastic tubules uniting and apoptosis (A) which gives rise to blind ending tubules, thereby effectively reducing the number of odontoblasts during their centripetal movement (arrows indicate the centripetal course followed by the odontoblasts, I - ivory).

Extreme care should be taken when harvesting ivory for chemical analyses. The proximal feather edge of the tusk as well as the layer of mineralised tissue ensheathing the tusk consists of cellular dental cementum and not ivory. Studies which provide no clarity on the exact part of the tusk that was harvested for chemical analyses, should be viewed with caution. During the formation of dentine (or ivory), which is essentially a hydroxyapatite deposited on an organic matrix, over 45 elements could potentially compete for incorporation (Wetherell & Robinson 1973). The inorganic composition of ivory reflects the composition of an animal's diet. Unlike bone, the composition of ivory remains stable and is not subjected to turnover and remodelling after formation thereof (Posner & Tannenbaum 1984). An extensive databank on the composition of ivory from different areas in Africa could assist in tracing the origin of ivory and might play a key role in identifying regions in which illegal ivory harvesting is taking place. This study as well as others (Van der Merwe *et al.* 1988, Van der Merwe *et al.* 1990, Vogel *et al.* 1990), clearly indicate the tracing of the source of ivory on its chemical composition to be a realistic possibility. The techniques used by these groups are expensive and the equipment used is not readily available. Our study indicated that the concentrations of calcium, phosphate, magnesium and fluoride are of potential value in identifying the site of origin of Southern African ivory. Addo, Etosha and Kaokoveld ivory in particular have unique compositions. Addo ivory was distinguished by its low calcium content and Kaokoveld and Etosha ivory by its high fluoride content.

The rapid rate of hydrolisation of ivory from the Kaokoveld and Etosha compared to other regions was of interest. The annual rainfall in these regions are low. The arid environment, characterised by dry savannah and shrub, has led to the term 'desert elephant' to those animals that were driven into the region by human inhabitation of the more arable land (Viljoen, 1987). There is good reason to accept that the diet of these elephant differ significantly from those in the other regions studied. Analyses of ivory from Kaokoveld and Etosha show the highest fluoride concentration, lowest total proline plus hydroxyproline content and under hydroxylation of lysine as unique characteristics. The high fluoride content is likely the result of the water that collects in the closed systems of salt pans and which becomes concentrated due to evaporation. Although excessive fluoride could influence the strength of the hydroxyapatite crystal (Lavelle 1975), the under-hydroxylation of lysine would affect the strength of the organic scaffold of collagen fibres (Chatterjee 1978). Vitamin C, iron and oxygen are cofactors required for the enzymatic hydroxylation of lysine during the biosynthesis of the tropocollagen molecule (Anderson 1992). Insufficient dietary Vitamin C intake, linked to the arid vegetation, is likely to be the main cause of reduced hydroxylation of lysine in the collagen of Kaokoveld and Etosha ivory.

Acknowledgements

The author wishes to thank Mrs C.S. Begemann for typographical support, the National Parks Board and in particular Dr V. De Vos for making the tusks and fragments of ivory available and the Department of Chemical Pathology and Electronmicroscope Unit at Medunsa for technical support. This study was supported by a grant from the Foundation for Research Development.

References

ANDERSON, J.C. 1992. Biochemical basis of connective tissue disease. Pp. 174 – 226. *In:* GARDNER, L. (ed.). *Pathological Basis of Connective tissue diseases.* Philadelphia: Lea & Febiger.

ARMSTRONG, S. & F. BRIDGLAND. 1989. Elephants and the ivory tower. *New Scientist* 124(1679):37–41.

CHATTERJEE, G.C. 1978. Nutritional deficiencies in animals: Vitamin C. Pp. 149–176. *In:* RECHCIGL, M. (ed.). *CRC Handbook series in nutrition and food, Section E: Nutritional Disorders.* Vol. 2. Florida: CRC Press.

LAVELLE, C.L.B. 1975. *Applied Physiology of the Mouth.* Bristol: John Wright.

MILES, A.E.W. & A. BOYDE. 1961. Observations on the structure of elephant ivory. *Journal of Anatomy (London)* 95:450.

POSNER, A.S. & P.J. TANNENBAUM. 1984. The mineral phase of dentine. Pp. 17–36. *In:* LINDE, A. (ed.). *Dentine and Dentinogenesis. Vol.2.* Florida: C.R.C. Press.

RAUBENHEIMER, E.J., J. DAUTH, M.J. DREYER, P.D. SMITH & M.L. TURNER. 1990. Structure and composition of ivory of the African elephant (*Loxodonta africana*). *South African Journal of Science* 86:192–193.

SIKES, S.K. 1971. *The natural history of the African elephant.* London: Weidenfeld and Nicholson.

SOGGNAES, R.F. 1960. The ivory core of tusks and teeth. *Journal of Clinical Orthopaedics* 17:43–61.

VAN DER MERWE, N.J., J.A. LEE THORPE & R.H.V. BELL. 1988. Carbon isotopes as indicators of elephant diets and African environments. *African Journal of Ecology* 26:163–172.

VAN DER MERWE, N.J., J.A. LEE THORPE, J.F. THACKERAY, A. HALL-MARTIN, F.J. KRUGER, H. COETZEE, R.H.V. BELL & M. LINDEQUE. 1990. Source area determination of elephant ivory by isotope analysis. *Nature* 346(6286): 744–746.

VILJOEN, P.J. 1987. Status and past and present distribution of elephants in the Kaokoveld, South West Africa Namibia. *South African Journal of Zoology* 22:247–257.

VOGEL, J.C., B. EGLINGTON & I.M. AURET. 1990. Isotope fingerprints in elephant bone and ivory. *Nature (London)* 346(6286): 747–749.

WETHERELL, J.A. & C. ROBINSON. 1973. The inorganic composition of teeth. P. 43. *In:* ZIPKIN, I. (ed.). *Biological Mineralization.* New York: Wiley.

Nuclear Instruments and Methods in Physics Research B 104 (1995) 638–644

NIM B
Beam Interactions with Materials & Atoms

ELSEVIER

Trace element concentration and distribution in ivory

V.M. Prozesky[a,*], E.J. Raubenheimer[b], W.F.P. Van Heerden[b], W.P. Grotepass[b], W.J. Przybylowicz[a,1], C.A. Pineda[c], R. Swart[d]

[a] *Van de Graaff Group, National Accelerator Centre, P.O. Box 72, 7131 Faure, South Africa*
[b] *Department of Oral Pathology and Oral Biology, Faculty of Dentistry, Medical University of South Africa, Garankua, South Africa*
[c] *Groote Schuur Hospital, P.O. Box 7925, Observatory, Cape Town, South Africa*
[d] *Department of Geology, Stellenbosch University, Stellenbosch, South Africa*

Abstract

The trace element content and distribution in ivory from elephants and hippopotami were measured for both natural elements and elements present due to pollution. The National Accelerator Centre Nuclear Microprobe was used to investigate trace elements heavier than Ca, and distributions of these trace elements were measured over small areas (ca. 1 mm^2), using the Dynamic Analysis imaging method in the GeoPIXE software package. Quantitativity of elemental maps was checked by complementary point analyses in the same area as where the elemental maps were taken from and found to be accurate to within around 10%. The possibility of locating ivory on the basis of the trace element concentrations, determined by the environment in which these animals live, was demonstrated by using correspondence analysis.

1. Introduction

Mineralised tissue from living organisms has been the subject of many studies with analytical techniques during the last few decades [1–7], as the composition and trace elements concentration and distribution is maintained over time. Other reasons are the relatively little sample preparation necessary for analysis, and the fact that thick samples can be analysed with relative ease, due to the fairly constant composition of the matrix. Teeth, in contrast with bone, can generally be considered to be representative of the in vivo matrix for a long time after extraction. Teeth with a matrix consisting of calcium hydroxy-apatite, and ivory in particular, offer excellent opportunities to study a part of the history of an animal over a period of time, and include elements which were part of the environment, whether present naturally or as pollutants added by man. As examples, this allowed the study of trace elements in human teeth with the aim of establishing causes and catalysts for diseases [4, 5] and the effects of pollutants such as Pb on mental health [2, 3, 6]. Teeth in animals have also been analysed, yielding information on the biological process of formation [7]. The environmental history of the subject may also be traced by using the trace elemental composition of the teeth.

Mammalian ivory is a very good example of such material, and this study was aimed at establishing the effect of the environment, such as vegetation, climate and geology, on the trace element composition of ivory, especially elephant, from bearers around Southern Africa and Siberia. These elements absorbed in the plant life and water, become incorporated in the diet of the animals, and are finally reflected in the tissue of the animal, including the ivory.

One of the difficulties in controlling the sales of elephant ivory is the problem of poaching, which has led both the elephant and rhinocerous to become endangered species. For this reason there is a total ban on the sales of ivory, even for countries with legal ivory stocks obtained from culling and natural death of elephants. The development of techniques for tracing the origin of ivory is therefore extremely important to allow authorities to establish the legality of ivory in the market. The determination of trace element concentrations could contribute to solve some of the above problems and this study was partly aimed to determine the possibility of localising ivory on the basis of trace element concentrations, as measured by the PIXE technique.

* Corresponding author.

[1] On leave from the Faculty of Physics and Nuclear Techniques, Academy of Mining and Metallurgy, Cracow, Poland.

SSDI 0168-583X(95)00471-8

A further advantage of determination of trace element concentrations in ivory, is the fact that environmental pollution might be detected in the ivory of bearers from different areas. The Eastern Transvaal in South Africa, which includes the Kruger National Park, is partly industrialised with most of these industries based on the extraction of minerals. The detection of heavy elements, which invariably end up in the rivers of these areas, also led to the study of pollution as a function of time and geographical area in ivory bearers. For example it has been shown before that the Olifants river has a F content 5 times higher than normally found in similar areas [8].

Although the PIXE technique has been applied successfully in many studies of teeth, the study of ivory has not received a lot of attention. Elephant and rhino ivory have previously been studied with NAA [9, 10], with the aim of localising ivory from different areas, based on different isotopic ratios (e.g. C, N and Sr) and concentrations of different trace elements. The technique uses the fact that the isotopic ratios and concentrations of elements vary from region to region, due to differences in the environmental conditions. In this pilot study nine trace elements were detected in samples of ashed and raw ivory samples. Samples from different regions could be separated with the aid of statistical packages, such as correspondence analysis, although the number of samples analysed was small, with insufficient statistical information.

2. Ivory and sample preparation

The ivory matrix consists of calcium-hydroxy-apatite (CHA), offering an excellent matrix for PIXE analysis of heavy elements. The CHA is partly formed as an amorphous and crystalline structure. A schematic of elephant ivory, with an indication of the growth direction, is indicated in Fig.1. The growth of the ivory is initiated in the pulpal cavity, and the tissue is transported in helical tubili to the growth sites, on the outside of the dentine. The site from where the samples were taken from, is indicated by a polygon.

The ivory samples were cut with a saw, and these surfaces were polished with diamond paste. Paste with grain sizes of 6 and 1 μm were used consecutively, with the resulting surface polished to a high quality. The diamond paste and polishing cloth were separately analysed to establish the possibility of contamination of the samples during polishing. The highest contribution to contamination was found for the diamond paste, with a Cu concentration of around 20 ppm. Considering the concentration of paste left on the surface after polishing, this was considered negligible. The samples were nevertheless then washed in distilled and demineralised water, and wiped dry with the same polishing cloth. Although the ivory samples did not produce significant charge-up problems during analysis, the samples were coated with a thin layer of carbon to ensure that conduction of beam charge was adequate.

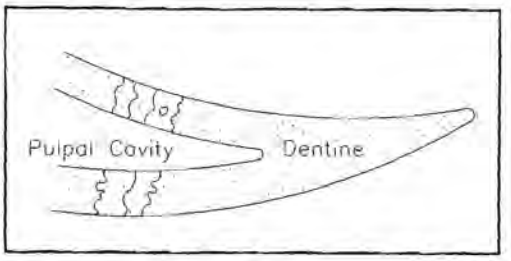

Fig. 1. A schematic of elephant ivory, with the growth direction indicated. The tissue for deposition is transported in the helical tubili for deposition on the outside of the dentine. The location where the samples analysed were taken from is also indicated.

3. Experimental

The Nuclear Microprobe (NMP) [11, 12] of the National Accelerator Centre (NAC) was used for the analysis. The beam energy selected was 3.0 MeV protons, and the X-rays were detected in an 80 mm^2 Si(Li) detector situated at 135°, with an energy resolution of 175 eV at 5.9 keV. The facility has been described before [11, 13], and details can be obtained from these references. Secondary electrons were maintained on the target using an electron suppression ring with a negative bias of 1500 V. The bulk of the X-rays from Ca were filtered out from the spectra using an 80 μm Al filter. All single point analyses were made with a total collected charge of 2.5 μC. These spectra were analysed using the GeoPIXE software package [14], with full thick target corrections applied. Elemental maps were also collected to study the variation of trace element concentrations as a function of position. The Dynamic Analysis (DA) method of mapping incorporated in this software package, in conjunction with the XSYS [12] data accumulation system, allowed the aquisition of true elemental maps during on-line analysis. The beam size used was around 10 × 10 μm, both for the line scans and the elemental mapping.

4. Results

4.1. Line scans and elemental maps

Care was exercised after it was found that some elements, such as Zn, were fairly mobile during beam bombardment. This was studied as a function of ion current and total dose, with the total dose alone showing no contribution to changes in any of the studied trace elements. The beam current was then optimised so as to

ensure no change in elemental concentrations, still ensuring that adequate detection limits could be obtained in a relatively short time. The beam current used was always around 5 nA.

A typical set of results for a few ivory samples are indicated in Table 1, with ivory from different geographical areas yielding different sets of concentrations. The table indicates the elements of interest, with the highest yield for trace elements obtained from Sr, which is biologically competing with Ca. A high yield for Fe was obtained for the Siberian ivory, values which were more than an order of magnitude larger than for all the other samples from other areas in Southern Africa. The lower limits of detection (LLD) were calculated using a 99% confidence interval, and the error values include a 3% filter error.

After establishing that the trace element concentrations were deviating on a relatively small scale in single ivory samples, line scans were made for different areas on the ivory. The results showed large deviations from most of the elements, with some of the results for a Siberian ivory specimen indicated in Fig. 2(a)–(c). In these figures the trace element concentration is indicated as a function of position, with the distance scale corresponding to 1.8 mm.

To eliminate the possibility of beam induced effects, the scan was made in both directions, the backward steps filling the gaps of the forward scan. Elements such as Mn, Zn and Sr showed the largest deviations, with maximum variations of up to 40% for Mn and Zn, and 12% for Sr.

These variations prompted the use of the elemental mapping facility of the GeoPIXE software package, and elemental maps were accumulated for a sample from the Kruger National Park. The scan size used was 1.3×1.3 mm. The resulting maps of Ca and Sr are indicated in Fig. 3 (a) and (b), showing marked variation in content as a function of position. The scales shown on the right-hand side of the maps are in ppm, and are the result of the quantitative mapping facility of GeoPIXE. Data presentation was made by the Interactive Data Language (IDL) package [15] and the maps are contours linking pixels with similar values.

The variations in these elements complement the line scan results, with large deviations in concentrations over a relatively small area. Although the samples analysed were too small to confirm ($< 3 \times 3$ mm), the results may show a 'tree ring' effect, of variations based on seasonal variations due to rain and plant differences. This is strengthened by comparing the growth rate of 2 mm per year for elephant ivory. There is also a positive correspondence with the Sr content of the light and dark bands optically seen in ivory, with dark areas containing significantly less Sr than the lighter areas. It is also clear that the concentrations of Sr and Ca are positively correlated.

Quantitativity of elemental maps was checked by complementary point analyses in the same area where

Table 1
A typical set of results of trace element concentrations for ivory samples from different geographical areas

Location	Fe	FeLLD	Zn	ZnLLD	Br	BrLLD	Sr	SrLLD	Ag	AgLLD	Pb	PbLLD
Siberia	2338 ± 147	3.8	49.0 ± 1.5	1.8	< LLD	1.5	710 ± 11.4	2.1	26.3 ± 3.0	4.4	12.9 ± 2.2	3.2
Kruger Park	6.7 ± 1.5	3.4	183 ± 5.6	2.4	2.1 ± 0.5	1.7	268 ± 4.5	2.0	21.3 ± 3.6	6.8	< LLD	3.9
Addo Park	48.1 ± 3.6	3.8	34.8 ± 1.6	2.0	3.8 ± 0.5	1.5	372 ± 6.7	2.2	19.1 ± 3.0	5.8	7.2 ± 1.5	3.4
Botswana	2.9 ± 1.4	4.2	39.3 ± 1.4	2.2	< LLD	1.7	143 ± 4.0	2.1	19.2 ± 3.2	7.0	< LLD	3.8
Namibia	9.1 ± 1.5	3.6	44.2 ± 1.7	2.4	3.5 ± 0.7	1.8	883 ± 16.7	2.2	35.6 ± 3.9	7.2	< LLD	4.2
North Natal	15.4 ± 1.9	3.6	37.5 ± 1.4	2.3	< LLD	1.8	350 ± 5.5	1.8	23.4 ± 4.4	6.8	< LLD	4.1
Hippo	7.9 ± 1.6	3.9	55.6 ± 1.9	2.7	3.1 ± 0.5	1.8	329 ± 6.0	2.1	23.3 ± 3.5	7.7	< LLD	4.5

Results are given in ppm.

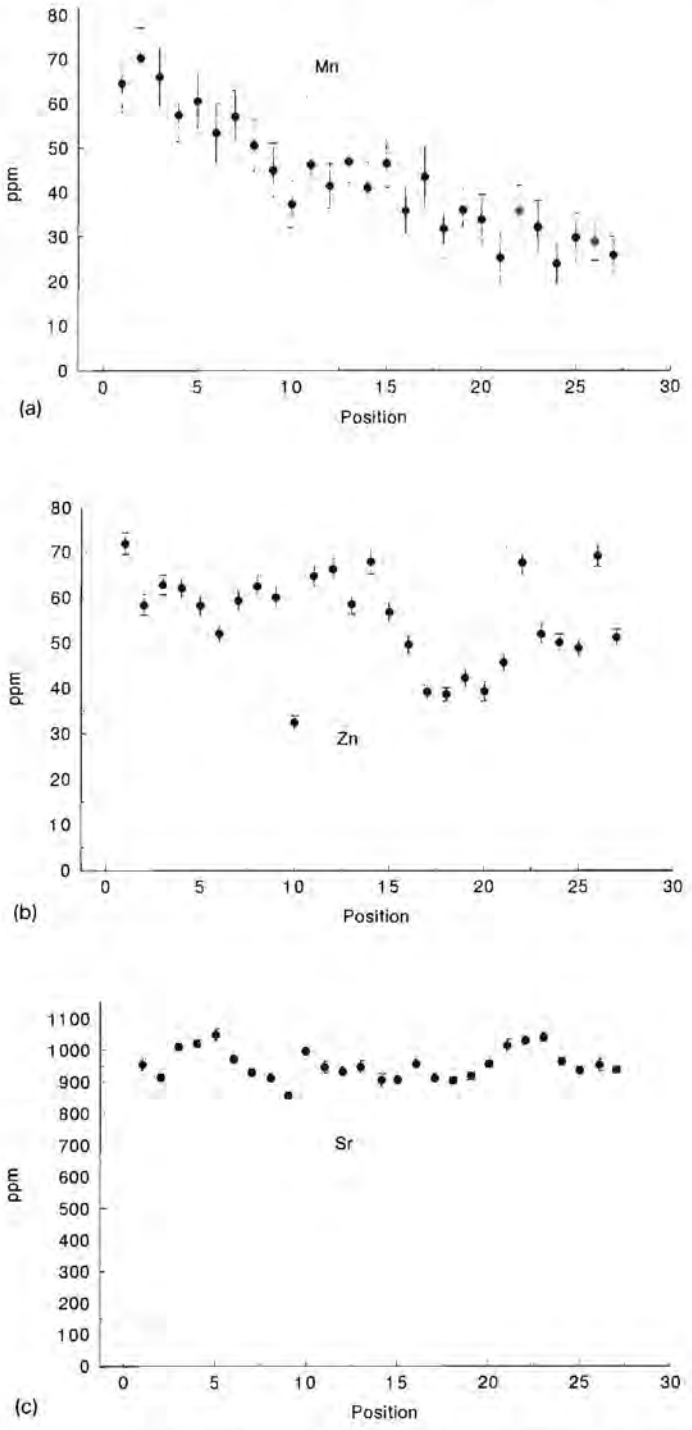

Fig. 2. Results of line scans across an ivory sample, indicating the changes in trace element concentrations for (a) Mn, (b) Zn and (c) Sr. The full scale of the X-axis is 1.8 mm. The points were analysed in both the forward and backward direction.

Results are given in ppm.

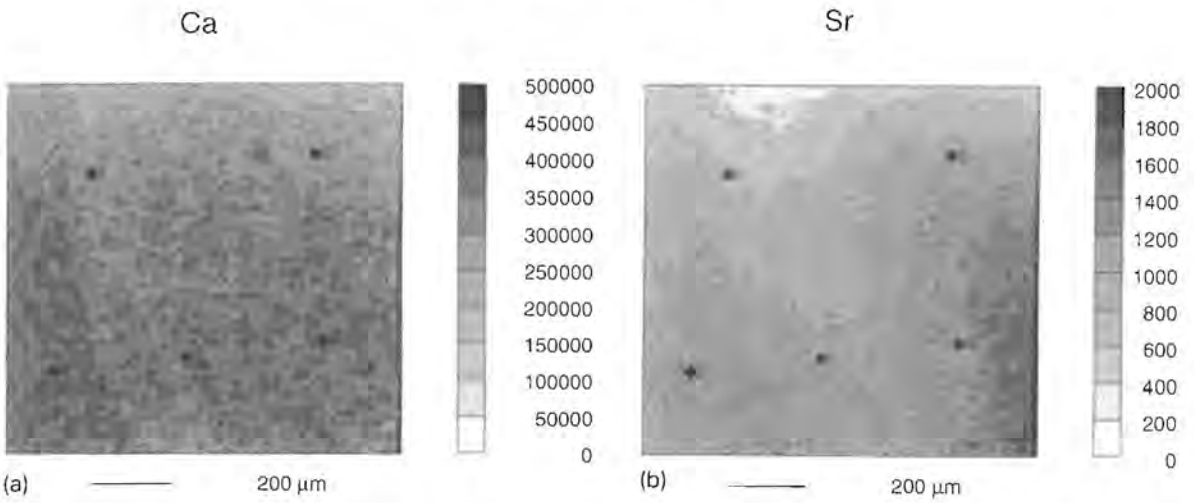

Fig. 3. Elemental maps (1.3 × 1.3 mm) for a sample from the Kruger National Park for (a) Ca and (b) Sr concentration. The intensity scale on the right-hand side of the maps are in ppm. The numbered dots on the maps are the spots analysed to compare with the mapping results. The comparisons are given in Table 2.

Table 2
Comparison of the results of the point analyses and mapping. The points are indicated as small numbered dots on the maps. The results of the mapping are given as the range of the pixel value at that specific spot in the map, compared to the accurate results of the point analyses. The numbers of the points are indicated in Fig. 3(a) and (b)

Position	Ca concentration (point) (%)	Ca concentration (map) (%)	Sr concentration (point) (ppm)	Sr concentration (map) (ppm)
1	34.9 ± 10.5	34.4 – 37.5	592 ± 9.0	625 – 750
2	40.7 ± 12.3	37.5 – 40.6	615 ± 11.4	625 – 750
3	33.7 ± 10.2	28.1 – 31.3	503 ± 9.5	500 – 625
4	39.0 ± 11.8	37.5 – 40.6	896 ± 16.3	1000 – 1125
5	26.5 ± 11.4	25.0 – 28.1	812 ± 13.3	875 – 1000

elemental maps were taken from. These points are indicated in Fig. 3(a) and (b) as small numbered dots. The comparison of results of point analyses and mapping results is shown in Table 2. The results of the mapping are given as the range of the pixel value at that specific spot in the map, compared to the results of the point analyses. The results compare favourably, and the mapping results typically agree within 10% of the accurate point analyses. The relatively large error bars of the Ca results are due to the 80 μm Al filter used to reduce the yield of Ca X-rays in the spectrum.

The results of Table 1 also showed no correlated enhancement of elements associated with pollution, such as Pb, Br and Ag. This might be due to the relatively low density of industries in areas with game parks, and might indicate that the rivers are not significantly polluted with heavy metals.

4.2. Point analyses

With the large variations obtained it is clear that the analysis of single points with a small beam size would yield erroneous results in attempting to determine the trace element concentrations in ivory. For this reason the beam was defocused to around 80 × 80 μm to allow the analysis of a more representative area of the ivory. In addition to this, three spots were analysed per sample, and the results averaged for final analysis. For this analysis a group of hippopotamus ivory was included. These animals were all from one area, and were considered to be a separate grouping, in addition to the elephant groupings.

From the results in Table 1, it is clear that the localisation of the ivory bearers could not be made by using one or two elements, and that more complex multivariate

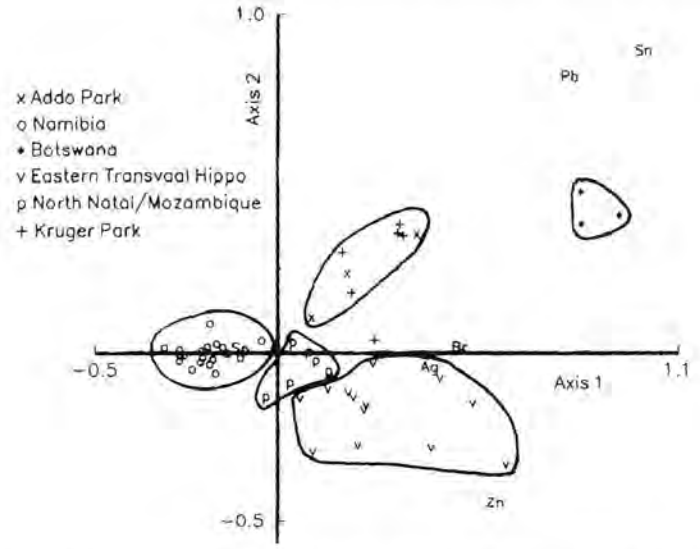

Fig. 4. Plot of the first two axes of the correspondence analysis data showing groupings of ivory from different geographical areas.

techniques should be used to include information on a variety of trace elements studied. The correspondence analysis package SIMCA [16] was used to group the results according to trace element concentration. The elements used were Zn, Br, Sr, Sn, Pb and Ag. The results of the statistical analysis are shown in Fig. 4. The grouping of the ivory is shown in two dimensions which contain almost 90% of the inertia, with the dimensions calculated on the basis of the trace element concentrations. Results from three pieces of ivory from Siberia are not included in the statistical analysis, as they are so far separated from the other results that they distort the scale. In Fig. 4 these results would be about −2.0 on Axis 1 and 0 on Axis 2. There is a strong correlation between the samples from the Kruger National Park and the Addo Park. It is not impossible, however, that elephants from the Kruger Park were relocated in the Addo Park, as such actions are executed from time to time. There is also one outlier in the Kruger Park results, that did not conform to the tight grouping of the rest of the Kruger Park samples. This sample, however, did not lead to overlap with other groups.

5. Conclusions

We have shown that trace element concentrations in ivory offer exciting results in terms of differences on a microscale, with environmental effects, such as season, water and plants, playing a role. It was also possible to localise ivory from different geographical areas with the aid of statistical correspondence analysis, showing trace element variation on the macroscale. These results offer new possibilities for localising ivory in trade, and might lead to the detection of poached ivory.

Acknowledgements

The authors gratefully acknowledge the cooperation of the South African Parks Board, and we thank them for the ivory supplied.

References

[1] M. Ahlberg and R. Akselsson, Int. J. Appl. Rad. Iso. 27 (1976) 279.
[2] B. Möller, L.E. Carlsson, G. Johansson, K.G. Malmqvist, L. Hammarström and M. Berlin, Scand. J. Work. Envir. Health 8 (1982) 267.
[3] K. Haavikko, A. Antilla, H. Helleland and E. Vuori, Arch. Envir. Health 37 (1984) 78.
[4] H.J. Annegarn, A. Jodaikin, P.E. Cleaton-Jones, J.P.F. Sellschop, C.C.P. Madiba and D. Bibby, Nucl. Instr. and Meth. 181 (1981) 323.
[5] I.D. Svalbe, M.A. Chaudri, K. Traxel, C. Ender and A. Mandel, Nucl. Instr. and Meth. B 3 (1984) 651.
[6] M.A. Chaudri and T. Ainsworth, Nucl. Instr. and Meth. 181 (1981) 333.
[7] G.W. Grime, F. Watt, S. Mann, C.C Perry, J. Webb and R.J.P. Williams, Trend. Biochem. Sci. 10 (1985) 6.
[8] E.J. Raubenheimer et al., South African J. Wildlife Res. 20 (4) (1990) 127.

[9] R.J. Hart, Annual Report of the Schonland Research Centre for Nuclear Sciences (1992) p. 30.
[10] R.J. Hart and M. Tredoux, Abstract in Nucl. Anal. Meth. Life Sci., Prague, Czech Republic, 13–17 September 1993.
[11] U.A.S. Tapper, W.R. McMurray, G.F. Ackermann, C. Churms, G. de Villiers, D. Fourie, P.J. Groenewald, J. Kritzinger, C.A. Pineda, J. Pilcher, H. Schmitt, K. Springhorn and T. Swart, Nucl. Instr. and Meth. B 77 (1993) 17.
[12] C.L. Churms, J.V. Pilcher, K.A. Springhorn and U.A.S. Tapper, Nucl. Instr. and Meth. B 77 (1993) 56.
[13] V.M. Prozesky et al., these Proceedings (ICNMTA '94), Nucl. Instr. and Meth. B 104 (1995) 36.
[14] C.G. Ryan and D.N. Jamieson, Nucl. Instr. and Meth. B 77 (1993) 203.
[15] Interactive Data Language, User's Manual, Version 3.1, RSI Inc., Boulder, USA.
[16] M.J. Greenacre, SIMCA – Version 2, PC Software for Correspondence Analysis (1990).